Chemorheological Relaxation, Residual Stress, and Permanent Set Arising in Radial Deformation of Elastomeric Hollow Spheres

HUGH E. HUNTLEY
Department of Mechanical Engineering, University of Michigan-Dearborn, Dearborn, MI 48128

ALAN S. WINEMAN
Department of Mechanical Engineering and Applied Mechanics, University of Michigan, Ann Arbor, MI 48109

K. R. RAJAGOPAL
Department of Mechanical Engineering, University of Pittsburgh, Pittsburgh, PA 15261

(Received 1 December 1995)

Abstract: Recently, a constitutive theory for rubber-like materials has been developed by which stress arises from different micromechanisms at different levels of deformation. For small deformations, the stress is given by the usual theory of rubber elasticity. As the deformation increases, there is scission of some junctions of the macromolecular microstructure. Junctions then reform to generate a new microstructure. The constitutive equation allows for continuous scission of the original junctions and formation of new ones as deformation increases. The macromolecular scission causes stress reduction, termed chemorheological relaxation. The new macromolecular structure results in permanent set on release of external load.

The present work considers a hollow sphere composed of such a material, also assumed to be incompressible and isotropic, which undergoes axisymmetric deformation under radial traction. There develops an outer zone of material with the original microstructure and an inner zone of material having undergone macromolecular scission, separated by a spherical interface whose radius increases with the deformation. The stress distribution, radial load-expansion response, residual stress distribution, and permanent set on release of traction are determined. It is found that a residual state of high compressive stress can arise in a thin layer of material at the inner boundary of the sphere.

1. INTRODUCTION

The general form of the constitutive equation for nonlinear elastic solids is based on assumptions that imply stress arises from a single unchanging material micromechanism at all stages of deformation. Rajagopal and Wineman [1] have recently presented a constitutive theory, which can be used to model the mechanical response of rubber-like materials that exhibit changes in micromechanism. In their model, the stress is determined by one micromechanism within some regime of deformation; as deformation increases,

Mathematics and Mechanics of Solids **1:** 267-299, 1996

a new micromechanism arises, which affects the mechanical response. They considered the particular example in which the material acts as a rubbery solid if the deformations are relatively small. When deformations become sufficiently large, some network junctions in the original material break and then reform to produce a new network with a new unstressed local configuration. Their work allowed for continuous conversion of the original material to new networks as deformation proceeds. It was shown that the material can undergo substantial softening and that there is permanent set when the applied load is removed. In the present article, the breakage of *network* junctions refers to the process of scission of the macromolecular microstructure. The reduction of stress due to this process is known as chemorheological relaxation (Tobolsky [2]) and is to be distinguished from the more familiar process of stress relaxation associated with macromolecular reconfiguration.

There have been several applications of this constitutive theory to problems involving nonhomogeneous deformations. The examples all assume that the material is incompressible and that new networks are generated at sufficiently large deformations. Wineman and Rajagopal [3] studied the finite extension and torsion of a circular cylinder. Huntley [4] considered the circumferential shear of a hollow concentric cylinder whose inner surface is fixed and whose outer surface is rotated about the centerline. Wineman and Huntley [5] studied a circular rubber membrane that is fixed at its boundary and subjected to a uniform pressure over one of its surfaces. Huntley, Wineman, and Rajagopal [6] analyzed the influence of this constitutive model on the monotonicity of the load-expansion behavior of thick-walled spheres. In each of these studies, when the deformation is sufficiently large, there is a region of original material separated from a region of multi-network material by an interface whose location varies with the size of the deformation. The ideas of [1] have been extended and generalized by Rajagopal and Srinivasa [7,8] to describe the twinning of metals and the inelastic response of materials in general.

The present work contains a detailed analysis of the response of a thick-walled sphere under radial traction. The regions of multi-network material and original material and their interface are determined as radial traction increases and then decreases. Stresses in these regions are also found. The chemorheological relaxation due to macromolecular scission reduces the maximum stress, as well as the radial traction required to impose a specified radial deformation. It is shown that there is a residual stress distribution and permanent set when the radial traction is removed.

The constitutive equation is presented in Section 2 and the equations governing the radial expansion of a hollow thick-walled sphere are presented in Section 3. The numerical method of solution is outlined in Section 4. Results for a numerical example are discussed in Section 5. The article concludes with remarks on special cases in Section 6.

2. CONSTITUTIVE EQUATION

Consider a sample of material undergoing a homogeneous deformation described by $\mathbf{x} = \mathbf{x}(\mathbf{X}, t)$, where $\mathbf{x}$ is the current position of a particle located at $\mathbf{X}$ in the undeformed

reference configuration, when $t = 0$. The deformation gradient associated with this mapping is $\mathbf{F} = \partial\mathbf{x}/\partial\mathbf{X}$ and the left Cauchy-Green tensor is given by $\mathbf{B} = \mathbf{F}\mathbf{F}^T$. Assume that there is a range of deformation on which the material behaves as an isotropic, incompressible, nonlinear Green elastic solid. It is well known (e.g., Spencer [9]) that the Cauchy stress $\mathbf{T}$ for this material takes the form

$$\mathbf{T} = -p\mathbf{I} + 2[W_1^{(1)}\mathbf{B} - W_2^{(1)}\mathbf{B}^{-1}], \tag{1}$$

where $-p\mathbf{I}$ is an indeterminate hydrostatic stress state. It will be convenient to denote the extra stress by $\mathcal{T} = \mathbf{T} + p\mathbf{I}$. $W^{(1)} = W^{(1)}(I_1, I_2)$ is the strain energy per unit volume, where $I_1 = \mathrm{tr}(\mathbf{B})$ and $I_2 = \mathrm{tr}(\mathbf{B^{-1}})$ are the first two invariants of $\mathbf{B}$. Also, $W_1^{(1)} = \partial W^{(1)}/\partial I_1$ and $W_2^{(1)} = \partial W^{(1)}/\partial I_2$.

An activation criterion determines when the original material network begins to undergo microstructural change and form new networks. This criterion is taken to be expressed as a function of the deformation gradient $\mathbf{F}$, which vanishes when microstructural change begins. Material frame indifference, isotropy, and incompressibility imply that the activation criterion can be expressed in terms of the invariants of $\mathbf{B}$: $A(I_1, I_2) = 0$.

Transformation of the original microstructural network is assumed to be continuous with increasing deformation. Introduce a scalar deformation state parameter s whose value is determined by the extent of deformation. It can be expressed in terms of the stretch invariants: $s = s(I_1, I_2)$. The value of s increases as deformation increases. No unique definition of the term *increasing deformation* is proposed. Instead, as in the previous applications of this constitutive equation ([3, 4, 5]), an appropriate form of s is selected for the deformation process under consideration. Recasting the activation criterion in terms of the state parameter gives $A(I_1, I_2) = s(I_1, I_2) - \dot{s}_a$. Microstructural conversion is initiated when the state parameter s first reaches the conversion-activation value s_a.

For $s < s_a$, no conversion has yet occurred; thus all material is original and the total stress is given by (1). At the current deformation state s, with $s \geq s_a$, stress in the remaining original material is also a function of the current deformation gradient $\mathbf{F}$.

Introduce the scalar-valued conversion rate function $a(s)$. As increasing deformation causes the state parameter to increase beyond $s = s_a$, the conversion rate function determines the amount of network transformation induced by additional deformation. The conversion rate function may have any form respecting the constraints $a(s) = 0, s < s_a$ and $a(s) \geq 0, s \geq s_a$. $a(s)$ must remain non-negative so that an increase in deformation always be associated with additional microstructural change. It is assumed that a is a continuous function of s.

Consider a value of the deformation state parameter $\hat{s} \geq s_a$. It is assumed that a network is formed at this value of the deformation state parameter. Its reference configuration is the configuration of the original material at state $\hat{s}$. It is assumed to be an unstressed configuration for the newly formed network. Stress in such a material network is a function of the subsequent deformation of the network relative to this unstressed configuration. Define the deformation gradient for the material formed at state

$\hat{s}$ as $\hat{\mathbf{F}} = \partial \mathbf{x}/\partial \hat{\mathbf{x}}$, where $\hat{\mathbf{x}}$ is the position of the particle in the configuration corresponding to deformation state $\hat{s}$. This gradient compares the neighborhood of a particle in the configuration at state s with the configuration of the new network when it was formed at state $\hat{s}$. The associated left Cauchy-Green tensor is given by $\hat{\mathbf{B}} = \hat{\mathbf{F}}\hat{\mathbf{F}}^T$.

Let it be assumed that the material network formed at state $\hat{s}$ is elastic, isotropic, and incompressible. The extra Cauchy stress at state s in a network formed at deformation state $\hat{s}$ then becomes

$$\mathcal{T}^{(2)} = 2[W_1^{(2)}\hat{\mathbf{B}} - W_2^{(2)}\hat{\mathbf{B}}^{-1}]. \tag{2}$$

Here, $W^{(2)} = W^{(2)}(\hat{I}_1, \hat{I}_2)$ is the strain energy density of the material formed at state $\hat{s}$ and subseqently deformed to state s. $\hat{I}_1$ and $\hat{I}_2$ are the appropriate invariants of $\hat{\mathbf{B}}$. The strain energy density functions $W^{(1)}$ and $W^{(2)}$ may be of any form. It is assumed that the single function $W^{(2)}$ governs the strain energy density in each newly formed network. The material defined by (1) and (2) should not be thought of as a simple material in the sense of Noll (see Rajagopal [10]).

Total current stress in the material is taken as the superposition of the contribution from the remaining material of the original network and the contributions from all networks formed at deformation states $\hat{s} \in [s_a, s]$. During a process of increasing deformation, the total current stress is given by

$$\mathbf{T} = -p\mathbf{I} + b(s)\mathcal{T}^{(1)} + \int_{s_a}^{s} a(\hat{s})\mathcal{T}^{(2)} d\hat{s}. \tag{3}$$

The function $b(s)$ is the volume fraction of the original network material remaining at state s, with $b(s) = 1, s \leq s_a$, and $b(s) \in [0,1], s \geq s_a$. The volume fraction $b(s)$ decreases as s increases. $\mathcal{T}^{(1)}$, found from (1), is the current stress in the remaining original material. The quantity $a(\hat{s})d\hat{s}$ may be interpreted as the volume fraction of material that ruptures and reforms as the deformation state increases from $\hat{s}$ to $\hat{s} + d\hat{s}$. $\mathcal{T}^{(2)}$, given by (2), is the stress in that portion of newly formed material. With (1) and (2), (3) can be written in the form

$$\mathbf{T} = -p\mathbf{I} + 2b(s)[W_1^{(1)}\mathbf{B} - W_2^{(1)}\mathbf{B}^{-1}] + 2\int_{s_a}^{s} a(\hat{s})[W_1^{(2)}\hat{\mathbf{B}} - W_2^{(2)}\hat{\mathbf{B}}^{-1}]d\hat{s}. \tag{4}$$

Equations (3) and (4) are constitutive equations for incompressible materials and respect the requirements of frame indifference.

Assume that the material has undergone a process of deformation whereby s has increased monotonically and that deformation is subsequently reduced, so that s decreases monotonically. Two assumptions are made concerning the process of decreasing deformation: (a) there is no further conversion of original material; (b) there is no reversal of microstructural transformation. These assumptions are made partly for analytical convenience. It may also be said, however, that any more complicated theory governing the reduction of deformation will only be useful when more information concerning real material behavior is available to guide its formulation.

The above requirements imply that $a(s) = 0$ as deformation is reduced. Thus the upper limit of the integral in (3) becomes fixed at $s = s^*$, the maximum value of the state

parameter reached during the process of increasing deformation. The volume fraction of original material remaining undergoes no further change, so that $b(s) = b(s^*)$ as deformation is reduced. The stress during a reduction of deformation from $s = s^*$ then has the form

$$\mathbf{T} = -p\mathbf{I} + b(s^*)\mathcal{T}^{(1)} + \int_{s_a}^{s^*} a(\hat{s})\mathcal{T}^{(2)}d\hat{s}, \tag{5}$$

where $\mathcal{T}^{(1)}$ is found from (1) and $\mathcal{T}^{(2)}$ is given by (2). Equation (5) can be written with (1) and (2) as

$$\mathbf{T} = -p\mathbf{I} + 2b(s^*)[W_1^{(1)}\mathbf{B} - W_2^{(1)}\mathbf{B}^{-1}] + 2\int_{s_a}^{s^*} a(\hat{s})[W_1^{(2)}\hat{\mathbf{B}} - W_2^{(2)}\hat{\mathbf{B}}^{-1}]d\hat{s}. \tag{6}$$

Equations (1), (4), and (6) represent the complete constitutive equation for all deformation processes.

Much of the notation to be used in this article has already been introduced. However, before proceeding to study the application of the constitutive equation, it is important that the notational scheme and the functional dependences that it implies be clearly understood. An overview of the principal elements of the notational system is presented here.

Unhatted kinematic quantities, such as $\mathbf{F}$, $\mathbf{B}$, I_1, and I_2, are referred to as *current* and compare configuration at the current deformation state s with the initial reference configuration. Kinematic quantities bearing the hat notation $\hat{(\ )}$, such as $\hat{\mathbf{F}}$, $\hat{\mathbf{B}}$, $\hat{I}_1$, and $\hat{I}_2$, are called *relative* quantities. They represent comparison of the configuration at the current state s with the configuration at state $\hat{s}$.

The superscript $(\ )^{(1)}$ appearing in stress quantities such as $\mathcal{T}^{(1)}$ indicates that the stress is in material of the original microstructural network. Such stresses are functions of the current left Cauchy-Green tensor $\mathbf{B}$. The superscript $(\ )^{(2)}$ appearing, for example, in $\mathcal{T}^{(2)}$ indicates stress in a material network formed at deformation state $\hat{s}$. These stresses are functions of the relative left Cauchy-Green tensor $\hat{\mathbf{B}}$. Unsuperscripted stresses, such as $\mathbf{T}$, are total stresses following the superposition given by (3) of stresses in original and newly formed networks. They are thus functions of the current tensor $\mathbf{B}$ and of the relative tensors $\hat{\mathbf{B}}$ relating the current configuration to each state $\hat{s} \in [s_a, s]$ for increasing deformation. For a process of increasing deformation, unsuperscripted stresses also depend explicitly on the current value of the deformation state parameter s, which appears as the upper limit of integration and as the argument of $b(s)$. During reversal of deformation, unsuperscripted stresses depend explicitly on s^*.

The function $W^{(1)}$ denotes the Helmholtz strain energy density in material of the original network; it is a function of the current stretch invariants I_1 and I_2. $W^{(2)}$ is the strain energy density in the material of a subsequently formed network and is a function of the relative invariants $\hat{I}_1$ and $\hat{I}_2$.

Nondimensionalized quantities bear the tilde notation $\tilde{(\ )}$, as $\tilde{\mathbf{T}}$.

For purposes of notational simplicity, none of the functional dependences mentioned above is indicated explicitly when kinematic or stress quantities are written.

3. FORMULATION

3.1. Kinematics of Deformation

Consider a sphere of initial outer radius R_o containing a central spherical cavity of radius R_i. In spherical coordinates, the undeformed sphere occupies the domain

$$D = \{(R, \Phi, \Theta) : R \in [R_i, R_o];\ \Phi \in [0, \pi];\ \Theta \in [0, 2\pi)\}. \tag{7}$$

No restriction is placed on the thickness of the sphere: all values of R_i and R_o, with $R_o > R_i$, are admissible. The sphere is considered to be composed of material that is initially homogeneous, incompressible, elastic, and isotropic.

Let T_o be a radial force per unit current surface area. A uniform radial tensile traction of magnitude T_o is applied at the outer surface. The surface of the inner cavity is traction-free. The resulting deformation is assumed to be spherically symmetric. With (r, ϕ, θ) denoting the current coordinates of the particle initially located at (R, Φ, Θ), the mapping describing the deformation has the form

$$\begin{aligned} r &= r(R) \\ \phi &= \Phi \\ \theta &= \Theta. \end{aligned} \tag{8}$$

The radial deformation function $r(R)$ is to be found. For the mapping given by (8), the general deformation gradient in spherical coordinates (e.g., [9]) is found to simplify to

$$\mathbf{F} = \mathbf{F}(R) = \operatorname{diag}\left(\frac{dr}{dR}, \frac{r}{R}, \frac{r}{R}\right). \tag{9}$$

The statement of incompressibility, $\det(\mathbf{F}) = 1$, may be written from (9) as

$$\left(\frac{r}{R}\right)^2 \frac{dr}{dR} = 1. \tag{10}$$

Introduce the notation $\lambda = r/R$. The incompressibility condition (10) becomes

$$\lambda^2 \frac{dr}{dR} = 1, \tag{11}$$

which gives $dr/dR = 1/\lambda^2$. Thus the current deformation gradient (9) with respect to the initial coordinates may be written as

$$\mathbf{F} = \operatorname{diag}\left(\frac{1}{\lambda^2}, \lambda, \lambda\right). \tag{12}$$

It can be seen from the deformation gradient (12) that each particle R of the sphere may be regarded as undergoing locally homogeneous equal biaxial extension. The r-, ϕ-

and θ-directions are the principal directions of stretch. There is no variation in deformation with the ϕ- and θ-coordinates; the state of equal biaxial extension is a function of the radial coordinate R.

The current left Cauchy-Green tensor and its inverse are found from (12) to be

$$\mathbf{B} = \mathbf{F}\mathbf{F}^T = \operatorname{diag}\left(\frac{1}{\lambda^4}, \lambda^2, \lambda^2\right) \tag{13}$$

and

$$\mathbf{B}^{-1} = \operatorname{diag}\left(\lambda^4, \frac{1}{\lambda^2}, \frac{1}{\lambda^2}\right). \tag{14}$$

The invariants of $\mathbf{B}$ are given by

$$I_1 = 2\lambda^2 + \frac{1}{\lambda^4}; \quad I_2 = \frac{2}{\lambda^2} + \lambda^4. \tag{15}$$

Note that (10) can be integrated to give the relation

$$\lambda = \lambda(R) = \left[1 + (\lambda_i^3 - 1)\left(\frac{R_i}{R}\right)^3\right]^{\frac{1}{3}}, \tag{16}$$

where λ_i denotes the equal biaxial stretch ratio $\lambda(R_i)$ at the inner surface of the sphere. Once the value of λ_i is specified, (16) gives the stretch ratio distribution $\lambda(R)$ for the entire sphere. The stretch ratio λ_i is thus considered a global deformation control parameter in the remainder of this article. It can be seen from (16) that, for a fixed particle label R, λ increases (or decreases) with λ_i. A process of increasing (or decreasing) λ_i thus assures a process of increasing (or decreasing) λ for all $R \in [R_i, R_o]$.

Recall the requirement that the deformation state parameter $s(I_1, I_2)$ increase with some measure of the stretch invariants. For $\lambda > 1$, both I_1 and I_2 as given by (15) increase monotonically in λ. Thus s can be expressed as $s(\lambda)$, a monotonically increasing function of λ. The parameter s also increases monotonically with λ_i at fixed R. Equation (16) also reveals that, for a fixed stretch λ_i, λ and hence s decrease monotonically as R increases.

Consider now the material of a particle R that undergoes conversion at some value of the deformation state parameter $\hat{s} \geq s_a$. Let $\hat{\lambda}$ be the equal biaxial stretch ratio corresponding to deformation state $\hat{s}$. It follows from (12) that

$$\frac{\partial \hat{\mathbf{x}}}{\partial \mathbf{X}} = \operatorname{diag}\left(\frac{1}{\hat{\lambda}^2}, \hat{\lambda}, \hat{\lambda}\right). \tag{17}$$

Deformation then increases beyond state $\hat{s}$. Note that

$$\hat{\mathbf{F}} = \mathbf{F}\left(\frac{\partial \hat{\mathbf{x}}}{\partial \mathbf{X}}\right)^{-1} \tag{18}$$

implies

$$\hat{\mathbf{F}} = \operatorname{diag}\left[\left(\frac{\hat{\lambda}}{\lambda}\right)^2, \frac{\lambda}{\hat{\lambda}}, \frac{\lambda}{\hat{\lambda}}\right]. \tag{19}$$

The relative left Cauchy-Green tensor and its inverse are formed from (19) as

$$\hat{\mathbf{B}} = \hat{\mathbf{F}}\hat{\mathbf{F}}^T = \text{diag}\left[\left(\frac{\hat{\lambda}}{\lambda}\right)^4, \left(\frac{\lambda}{\hat{\lambda}}\right)^2, \left(\frac{\lambda}{\hat{\lambda}}\right)^2\right] \tag{20}$$

and

$$\hat{\mathbf{B}}^{-1} = \text{diag}\left[\left(\frac{\lambda}{\hat{\lambda}}\right)^4, \left(\frac{\hat{\lambda}}{\lambda}\right)^2, \left(\frac{\hat{\lambda}}{\lambda}\right)^2\right]. \tag{21}$$

The relative invariants are found from (20) to be

$$\hat{I}_1 = 2\left(\frac{\lambda}{\hat{\lambda}}\right)^2 + \left(\frac{\hat{\lambda}}{\lambda}\right)^4; \quad \hat{I}_2 = 2\left(\frac{\hat{\lambda}}{\lambda}\right)^2 + \left(\frac{\lambda}{\hat{\lambda}}\right)^4. \tag{22}$$

3.2. Stress-Stretch Relations

Consider a process in which λ_i increases monotonically. As discussed above, the stretch ratio λ and hence the deformation state parameter s increase monotonically for all $R \in [R_i, R_o]$.

For any particle R that has not undergone microstructural transformation, where $s < s_a$, the nonzero current Cauchy stresses are given by (1), (13), and (14) as

$$\begin{aligned} T_{rr} &= -p + 2\left[\frac{W_1^{(1)}}{\lambda^4} - W_2^{(1)}\lambda^4\right] \\ T_{\theta\theta} &= -p + 2\left[W_1^{(1)}\lambda^2 - \frac{W_2^{(1)}}{\lambda^2}\right], \end{aligned} \tag{23}$$

with p an indeterminate scalar. Also, $T_{\phi\phi} = T_{\theta\theta}$. Note that, because the stretch tensors are diagonal, all shear stress components are identically zero. From (23) it is clear that the extra stress components are functions of λ. As discussed above, however, $\lambda(R)$ is given by (16) at any level of deformation of the sphere, once the deformation control parameter λ_i is prescribed. Thus the extra stresses may also be considered functions of the reference coordinate R.

The normal stress difference, $\bar{T} = \bar{T}(R) = T_{\theta\theta}(R) - T_{rr}(R)$, is of primary interest. From (23), the stress difference when $s < s_a$ is seen to be

$$\bar{T} = \bar{T}^{(1)} = 2E^{(1)}\left(\lambda^2 - \frac{1}{\lambda^4}\right), \tag{24}$$

where $E^{(1)}$ is the deformation-dependent modulus of the original material given by

$$E^{(1)} = E^{(1)}(\lambda(R)) = W_1^{(1)} + \lambda^2 W_2^{(1)}. \tag{25}$$

As λ_i increases, particles at some R may stretch to such an extent that $s(\lambda(R)) \geq s_a$. For particles with $s \geq s_a$, the nonzero current Cauchy stresses are formed from (4), (13), (14), (20), and (21) as

$$T_{rr} = -p + 2b(s)\left[W_1^{(1)}\frac{1}{\lambda^4} - W_2^{(1)}\lambda^4\right] + 2\int_{s_a}^{s} a(\hat{s})\left[W_1^{(2)}\left(\frac{\hat{\lambda}}{\lambda}\right)^4 - W_2^{(2)}\left(\frac{\lambda}{\hat{\lambda}}\right)^4\right] d\hat{s}$$

$$T_{\theta\theta} = -p + 2b(s)\left[W_1^{(1)}\lambda^2 - W_2^{(1)}\frac{1}{\lambda^2}\right] + 2\int_{s_a}^{s} a(\hat{s})\left[W_1^{(2)}\left(\frac{\lambda}{\hat{\lambda}}\right)^2 - W_2^{(2)}\left(\frac{\hat{\lambda}}{\lambda}\right)^2\right] d\hat{s}. \tag{26}$$

Again, $T_{\phi\phi} = T_{\theta\theta}$. The normal stress difference for $s \geq s_a$ is found from (26) to be

$$\bar{T} = 2\left\{b(s)E^{(1)}\left(\lambda^2 - \frac{1}{\lambda^4}\right) + \int_{s_a}^{s} a(\hat{s})E^{(2)}\left[\left(\frac{\lambda}{\hat{\lambda}}\right)^2 - \left(\frac{\hat{\lambda}}{\lambda}\right)^4\right] d\hat{s}\right\}, \tag{27}$$

with the deformation-dependent modulus of the newly formed material given by

$$E^{(2)} = E^{(2)}\left(\frac{\lambda}{\hat{\lambda}}\right) = W_1^{(2)} + \left(\frac{\lambda}{\hat{\lambda}}\right)^2 W_2^{(2)}. \tag{28}$$

Assume now that the sphere has undergone a process of increasing deformation whereby the deformation control parameter has reached a maximum value of $\lambda_i = \lambda_i^*$. Let $s^* = s^*(\lambda(R))$ denote the distribution of the deformation state parameter corresponding to $\lambda_i = \lambda_i^*$. The control parameter λ_i is subsequently decreased from λ_i^*. It follows from (16) that this constitutes a process of decreasing deformation λ for all $R \in [R_i, R_o]$. At any particle R for which $s^* < s_a$, no conversion has occurred. Cauchy stresses during reduction of deformation follow the form of (23) and the stress difference is given by (24). Any particle R for which $s^* \geq s_a$ has undergone some degree of network conversion. Stress components at such a particle during reduction of deformation are formed from (6), (13), (14), (20), and (21) as

$$T_{rr} = -p + 2b(s^*)\left[W_1^{(1)}\frac{1}{\lambda^4} - W_2^{(1)}\lambda^4\right] + 2\int_{s_a}^{s^*} a(\hat{s})\left[W_1^{(2)}\left(\frac{\hat{\lambda}}{\lambda}\right)^4 - W_2^{(2)}\left(\frac{\lambda}{\hat{\lambda}}\right)^4\right] d\hat{s}$$

$$T_{\theta\theta} = -p + 2b(s^*)\left[W_1^{(1)}\lambda^2 - W_2^{(1)}\frac{1}{\lambda^2}\right] + 2\int_{s_a}^{s^*} a(\hat{s})\left[W_1^{(2)}\left(\frac{\lambda}{\hat{\lambda}}\right)^2 - W_2^{(2)}\left(\frac{\hat{\lambda}}{\lambda}\right)^2\right] d\hat{s}, \tag{29}$$

with $T_{\phi\phi} = T_{\theta\theta}$. The normal stress difference is formed from (29) as

$$\bar{T} = 2\left\{b(s^*)E^{(1)}\left(\lambda^2 - \frac{1}{\lambda^4}\right) + \int_{s_a}^{s^*} a(\hat{s})E^{(2)}\left[\left(\frac{\lambda}{\hat{\lambda}}\right)^2 - \left(\frac{\hat{\lambda}}{\lambda}\right)^4\right] d\hat{s}\right\}. \tag{30}$$

Because $s = s(\lambda)$ and $\lambda = \lambda(R)$ by (16), each value of λ_i determines a variation of s with R. The state parameter s decreases monotonically with R for all λ_i. Figure 1 shows the general form of the s-R distribution for the sphere at several levels of deformation λ_i. At a low value of $\lambda_i = \lambda_{sm}$, $s < s_a$ for all $R \in [R_i, R_o]$, as seen in Figure 1. No microstructural change has occurred; the entire sphere is composed of the original material. Due to the one-to-one correspondence between s and λ, there exists a specific value of λ_i denoted by $\lambda_i = \lambda_a$, with $\lambda_a > \lambda_{sm}$, which corresponds to $s(\lambda_i) = s_a$. Conversion is just initiated at $R = R_i$; $s < s_a$ for all $R \in [R_i, R_o]$. When $\lambda_i = \lambda_{lg}$, where $\lambda_{lg} > \lambda_a$, there is an activation radius R_a defined by $s(\lambda(R_a)) = s_a$, where $\lambda(R_a) = \lambda_a$. Then $s > s_a$ for $R \in [R_i, R_a]$, while $s < s_a$ for $R \in [R_a, R_o]$. Thus there is an inner spherical region where conversion is taking place and both original material and newly formed networks are present and an outer spherical region composed purely of original material.

The activation value of the stretch ratio λ_a and the activation radius R_a are related by (16). With the substitutions $\lambda = \lambda_a$ and $R = R_a$, (16) can be rearranged to give

$$R_a = R_i \left(\frac{\lambda_i^3 - 1}{\lambda_a^3 - 1} \right)^{\frac{1}{3}}. \tag{31}$$

When λ_a is specified, it is clear from (31) that R_a moves outward as λ_i increases during a process of increasing deformation.

The Cauchy stresses for the inner region undergoing microstructural change, $R \in [R_i, R_a]$, are given by (26). Stresses in the outer region of original material, $R \in [R_a, R_o]$, are given by (23). Note that $R = R_a$ belongs to both of the two closed intervals on R. This holds because the results given by the two stress models (23) and (26) are identical at $R = R_a$.

Consider now the process of reduction of deformation from a maximum value of the control parameter $\lambda_i = \lambda_i^*$. Equation (31) indicates that the radius $R = R_a$ decreases with λ_i. This establishes that the activation radius cannot move outward during a process of decreasing deformation. The greatest value of R_a reached is that corresponding to the maximum stretch λ_i^*. This value, denoted by R_a^*, is given by (31) as

$$R_a^* = R_i \left(\frac{\lambda_i^{*3} - 1}{\lambda_a^3 - 1} \right)^{\frac{1}{3}}. \tag{32}$$

For the process of reduction of deformation, then, R_a^* defines the interface between the inner zone $R \in [R_i, R_a^*]$, where conversion has taken place and both original material and subsequently formed networks are present, and the outer region $R \in [R_a^*, R_o]$ of purely original material.

If the maximum value of the deformation control parameter is $\lambda_i^* < \lambda_a$, then R_a^* is undefined, as no network conversion has occurred anywhere on $[R_i, R_o]$. The stress components (23) and the stress difference (24) apply as deformation is reduced from $\lambda = \lambda_i^*$.

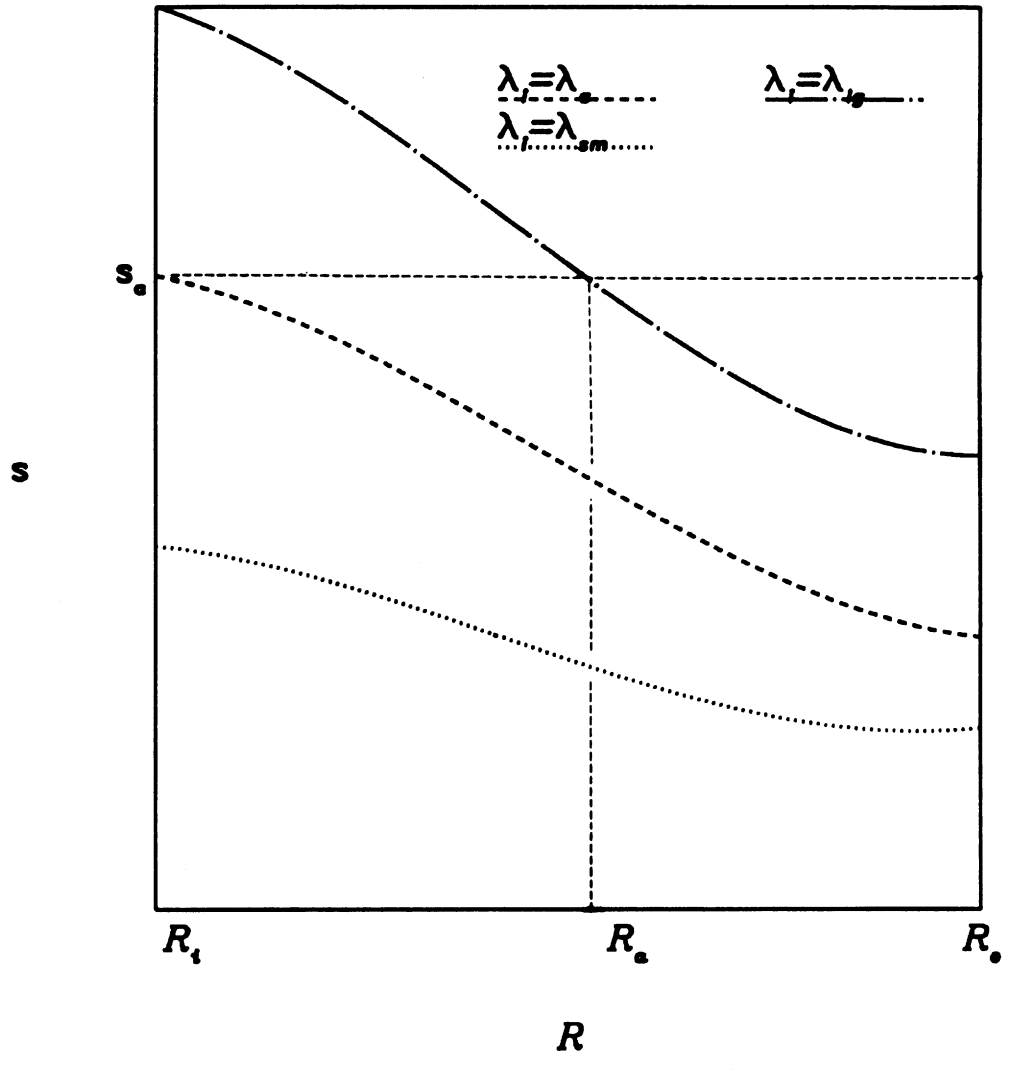

Fig. 1. Typical forms of deformation state parameter versus radius for various inner surface stretch ratios; activation radius is indicated for $\lambda_i = \lambda_{lg}$.

When the maximum stretch λ_i^* imposed during the process of increasing deformation is given by $\lambda_i^* \geq \lambda_a$, then there exists an $R_a^* \in [R_i, R_o]$ given by (32). As deformation decreases, stresses in material on $[R_a^*, R_o]$ follow (23) and (24). For material on $[R_i, R_a^*]$, the Cauchy stress components are given by (29) and the normal stress difference by (30).

3.3. Equilibrium

It should be noted that the spherical deformation described by (8) is a controllable deformation (Carroll [11]). For any incompressible isotropic solid, a scalar field p can be found, which satisfies the equilibrium equations. Furthermore, it can be shown that $p = p(r)$.

It has been shown that the shear components of the Cauchy stress are identically zero and that the extra stresses $\mathcal{T}_{rr}$ and $\mathcal{T}_{\phi\phi} = \mathcal{T}_{\theta\theta}$ are independent of the coordinates ϕ and θ. When body forces are neglected, and use is made of $T_{\phi\phi} = T_{\theta\theta}$, the equilibrium equations in spherical coordinates (e.g., [9]) are reduced to

$$\frac{dT_{rr}}{dr} + 2\,\frac{T_{rr} - T_{\theta\theta}}{r} = 0. \tag{33}$$

It may be observed from (16) that the mapping from R to r is one-to-one. Therefore, the statement of equilibrium (33) can be expressed in terms of the reference coordinate R as

$$\frac{dT_{rr}}{dR} + 2\,\frac{T_{rr} - T_{\theta\theta}}{R\lambda^3} = 0, \tag{34}$$

where $\lambda = r/R$ and (11) have been used. Written in terms of the normal stress difference, (34) becomes

$$\frac{dT_{rr}}{dR} - 2\,\frac{\bar{T}}{R\lambda^3} = 0. \tag{35}$$

Because the deformation is controllable, the equilibrium condition (35) is satisfied at every point $R \in [R_i, R_o]$ and at every value of the deformation control parameter λ_i.

The radial normal stress T_{rr} must be continuous and have a continuous first derivative dT_{rr}/dR on $[R_i, R_o]$. In particular, these quantities must be continuous at the interface $R = R_a$ between the inner region of converting material and the outer region composed entirely of original material. Comparison of the expressions (23) and (26) confirms that the extra stresses $\mathcal{T}_{rr}$ and $\mathcal{T}_{\theta\theta}$ are continuous at $R = R_a$ for any form of $a(s)$. It can be shown from (16), (23), (26), and (35) that $a(s_a) = 0$ and $db/ds = 0$ at $s = s_a$ are sufficient conditions for continuity of dT_{rr}/dR at $R = R_a$. These conditions will be enforced through appropriate selection of $a(s)$ and $b(s)$.

The equations for $p = p(R)$ are now presented, as they are needed for the calculation of the normal stresses T_{rr} and $T_{\theta\theta}$. The inner surface of the sphere at $R = R_i$ is considered free of traction, which gives the boundary condition $T_{rr}(R_i) = 0$. Using this condition and $T_{rr} = -p + \mathcal{T}_{rr}$, integration of (35) gives

$$p = \mathcal{T}_{rr} - 2\int_{R_i}^{R} \frac{\bar{T}}{\check{R}\lambda^3}\,d\check{R}. \tag{36}$$

When $\lambda_i < \lambda_a$, it follows that $s < s_a$ for all $R \in [R_i, R_o]$. Equation (36) is thus written using $\mathcal{T}_{rr} = \mathcal{T}_{rr}^{(1)}$ as found from (23) and $\bar{T} = \bar{T}^{(1)}$ as given by (24). These are the radial extra stress and normal stress difference expressions for untransformed original material.

When $\lambda_i \geq \lambda_a$, the activation radius R_a is given by (31). Recalling that $s \geq s_a$ on $R \in [R_i, R_a]$, p there follows the form (36), with $\mathcal{T}_{rr}$ found from (26) and $\bar{T}$ given by (27). These are the radial extra stress and the normal stress difference in material undergoing network conversion. On $[R_a, R_o]$, p takes the form

$$p = \mathcal{T}_{rr}^{(1)} - 2\left[\int_{R_i}^{R_a} \frac{\bar{T}}{\check{R}\lambda^3} d\check{R} + \int_{R_a}^{R} \frac{\bar{T}^{(1)}}{\check{R}\lambda^3} d\check{R}\right]. \tag{37}$$

$\mathcal{T}_{rr}^{(1)}$, found from (23), is the radial extra stress in the purely original material found on $[R_a, R_o]$; $\bar{T}^{(1)}$, as given by (24), is the normal stress difference in the material of this unconverted outer region. $\bar{T}$, given by (27), is the normal stress difference for $R \in [R_i, R_a]$, where both original material and newly formed networks contribute to the response.

When the sphere is subjected to a process of reduction of deformation from a maximum of $\lambda_i^* < \lambda_a$, p is given by (36) for all $R \in [R_i, R_o]$, with $\mathcal{T}_{rr} = \mathcal{T}_{rr}^{(1)}$ from (23) and $\bar{T} = \bar{T}^{(1)}$ from (24). When $\lambda_i^* \geq \lambda_a$, p on $R \in [R_i, R_a^*]$ is found from (36), with $\mathcal{T}_{rr}$ now found from (29) and $\bar{T}$ given by (30). For $R \in [R_a^*, R_o]$, p is given by (37), where $\mathcal{T}_{rr}^{(1)}$ is found from (23) and $\bar{T}^{(1)}$ is given by (24) and $\bar{T}$ by (30).

3.4. Load-Expansion Relation

Let (35) be integrated form R_i to R_o. Imposing the boundary conditions that the surface of the inner cavity be traction-free and the uniform radial tensile traction at the outer surface be T_o gives the result

$$T_o = 2\int_{R_i}^{R_o} \frac{\bar{T}}{R\lambda^3} dR. \tag{38}$$

When $\lambda_i < \lambda_a$, $s < s_a$ for $R \in [R_i, R_o]$ and T_o is found from (38), with $\bar{T} = \bar{T}^{(1)}$ given by (24). If $\lambda_i \geq \lambda_a$, microstructural transformation has been activated and $s \geq s_a$ on the inner region of the sphere $R \in [R_i, R_a]$. The external traction is then

$$T_o = 2\left[\int_{R_i}^{R_a} \frac{\bar{T}}{R\lambda^3} dR + \int_{R_a}^{R_o} \frac{\bar{T}^{(1)}}{R\lambda^3} dR\right]. \tag{39}$$

$\bar{T}$ is the current stress difference in material undergoing conversion and is given by (27). Note from (24) and (27) that $\bar{T}$ is determined at each particle R by the current value of $\lambda(R)$ and the history of $\lambda(R)$. During a process of monotonically increasing deformation, this history is identical for particles sharing a specified current value of λ. Furthermore, the distribution $\lambda(R)$ is determined by λ_i and R_i in (16). Thus, with R_o specified, it follows from (38) that $T_o = T_o(\lambda_i)$, a relation between the traction at the outer surface and the equal biaxial stretch ratio at the inner surface of the sphere.

Consider the process whereby λ_i has been increased to a maximum value of λ_i^* and subsequently decreased. When $\lambda_i^* < \lambda_a$, the external traction T_o during this process of reduction of deformation is given by (38) and (24). If $\lambda_i^* \geq \lambda_a$, T_o is found from (39), with $\bar{T}^{(1)}(R)$ given by (24) and $\bar{T}(R)$ by (30).

In the context of the spherical geometry, let the residual deformation be defined by the value of the deformation control parameter λ_i^{res} when the external traction T_o has been returned to zero, that is, $T_o(\lambda_i^{res}) = 0$. When $\lambda_i^* < \lambda_a$, (24) and (38) can be used to show that there is no residual deformation, so that $\lambda_i^{res} = 1$. For $\lambda_i^* \geq \lambda_a$, it is expected that $\lambda_i^{res} > 1$, with the corresponding residual stretch distribution

$$\lambda^{res} = \lambda^{res}(R) = \left\{1 + \left[(\lambda_i^{res})^3 - 1\right]\left(\frac{R_i}{R}\right)^3\right\}^{\frac{1}{3}}. \tag{40}$$

The condition that $T_o(\lambda_i^{res}) = 0$, together with (39), implies that

$$\int_{R_i}^{R_a^*} \frac{\bar{T}}{R(\lambda^{res})^3} dR + \int_{R_a^*}^{R_o} \frac{\bar{T}^{(1)}}{R(\lambda^{res})^3} dR = 0, \tag{41}$$

where $\bar{T}^1 = \bar{T}^1(\lambda^{res}(R))$ is formed from (24) and $\bar{T} = \bar{T}(\lambda^{res}(R))$ from (30). With (40), (41) becomes an integral equation for λ_i^{res}. It appears that numerical solutions for specific cases are the only means to precise information about λ_i^{res}.

4. NUMERICAL SOLUTION

To carry out a numerical solution, specific choices must be made for two material properties – the deformation state function s and the conversion rate function $a(s)$ introduced in (3). The deformation state function is chosen as $s = \lambda$ for $\lambda \geq 1$. The stretch ratio varies with the radius R, as does the state parameter; hence $s(R) = \lambda(R)$. The conversion activation criterion is satisfied for the particle at radius R when $s(R) = \lambda(R) = \lambda_a$. The activation radius, then, is defined by $\lambda(R_a) = \lambda_a$.

The conversion rate function $a(\lambda) = a(s)$ is chosen to be quadratic on a finite domain:

$$a(\lambda) = \begin{cases} 0, & \lambda < \lambda_a \\ \alpha(\lambda - \lambda_a)(\lambda - \lambda_c), & \lambda \in [\lambda_a, \lambda_c] \\ 0, & \lambda > \lambda_c. \end{cases} \tag{42}$$

According to this definition of $a(\lambda)$, the process of material conversion occurs as the deformation state parameter λ increases over a finite interval and the process terminates when $\lambda > \lambda_c$. Since the deformations under consideration are finite, the parameter λ will not exceed some finite value. Thus λ_c can be chosen sufficiently large that, in the present examples, the conversion process need not reach completion. (It should be noted that other choices of $a(\lambda)$ can be made in which λ_c is not finite.)

For simplicity, assume that the rate of decrease of volume fraction of original material equals the rate of increase of volume fraction of material with new microstructure. This implies that the volume fraction of original material remaining at any state of deformation $\lambda > \lambda_a$ is

$$b(\lambda) = 1 - \int_{\lambda_a}^{\lambda} a(\hat{\lambda}) d\hat{\lambda}. \tag{43}$$

With $a(\lambda)$ chosen as in (42) and $b(\lambda)$ chosen as in (43), the continuity condition for dT_{rr}/dR at $R = R_a$ is satisfied. Let the total volume fraction of material that may ultimately convert be denoted by C, where $C \leq 1$. Then by (43),

$$C = \int_{\lambda_a}^{\lambda_c} a(\hat{\lambda}) d\hat{\lambda}. \tag{44}$$

It then follows from (42) and (44) that

$$\alpha = -\frac{6C}{(\lambda_c - \lambda_a)^3}. \tag{45}$$

Values of λ_a, λ_c, and C are selected so as to make evident the differences in response between the sphere undergoing conversion and an elastic sphere (no conversion, $C = 0$). For the examples in this section, λ_a is chosen to be 1.5 so that network conversion commences at a relatively low level of deformation. It is desired to continue the simulation to the level $\lambda = 6.0$. Thus $\lambda_c = 6.1$ is chosen. This permits the simulation to demonstrate the effects of conversion of nearly all of the material specified by C while not exceeding λ_c.

Define a dimensionless radial coordinate by $\tilde{R} = R/R_i$. The equation (16) giving the stretch distribution becomes

$$\lambda = \lambda(\tilde{R}) = \left(1 + \frac{\lambda_i^3 - 1}{\tilde{R}^3}\right)^{\frac{1}{3}}. \tag{46}$$

When λ_i is specified, λ is a monotonically decreasing function of $\tilde{R}$. The numerical examples presented below assume a sphere occupying the reference domain $\tilde{R} \in [1.0, 10.0]$. The dimensionless outer radius of the sphere, denoted by $\tilde{R}_o = R_o/R_i$, is thus $\tilde{R}_o = 10$. The dimensionless activation radius $\tilde{R}_a = R_a/R_i$ is given by

$$\tilde{R}_a = \left(\frac{\lambda_i^3 - 1}{\lambda_a^3 - 1}\right)^{\frac{1}{3}}. \tag{47}$$

Here, $\tilde{R}_a$ is undefined for $\lambda_i < \lambda_a$. $\tilde{R}_a$ moves outward through the sphere for increasing $\lambda_i \geq \lambda_a$. At large λ_i, the plot of $\tilde{R}_a$ versus λ_i asymptotically approaches the straight line $\tilde{R}_a = \lambda_i(\lambda_a^3 - 1)^{-\frac{1}{3}}$.

The stress components T_{rr}, $T_{\phi\phi}$, and $T_{\theta\theta}$, the normal stress difference $\bar{T}$, and the traction T_o are normalized by an elastic constant appropriate to the material model being

considered. This gives dimensionless stresses denoted by $\tilde{T}_{rr}$, $\tilde{T}_{\phi\phi}$, $\tilde{T}_{\theta\theta}$, $\tilde{T}$, and $\tilde{T}_o$, respectively. A dimensionless scalar field $\tilde{p}$ is formed in the same way.

The numerical procedure for the solution begins with the specification of a value of the deformation control parameter λ_i. Then $\lambda(\tilde{R})$ is known everywhere from (46). With the activation stretch ratio λ_a prescribed, (47) gives $\tilde{R}_a$. Using the quadratic form of $a(\lambda)$ specified in (42), the integral in the equation (26) for the Cauchy stress components can be expanded analytically. Thus all extra stresses are calculated explicitly from (26) for $\tilde{R} \in [1, \tilde{R}_a]$ or from (23) for $\tilde{R} \in [\tilde{R}_a, \tilde{R}_o]$.

To calculate the scalar field $\tilde{p}$, the region $[1, \tilde{R}_a]$ is discretized to form n intervals of equal size demarcated by the nodes $\tilde{R} = R_j$ $(j = 1, n+1)$, with $R_1 = 1$ and $R_{n+1} = \tilde{R}_a$. Similarly, discretization of the region $[\tilde{R}_a, \tilde{R}_o]$ into m intervals is accomplished with the evenly spaced nodes $\tilde{R} = R_j$ $(j = 1, m+1)$, with $R_1 = \tilde{R}_a$ and $R_{m+1} = \tilde{R}_o$. The integrand of (26) is then evaluated at the nodal values R_j and the integral is approximated by Simpson's rule. The two distinct discretized regions are necessary because, as is known from (37), different forms of $\tilde{T}$ apply in the separate regions. When $\lambda_i \geq \lambda_a$, the numerical integration must be carried out from $\tilde{R} = 1$ precisely to $\tilde{R} = \tilde{R}_a$ using $\tilde{T}$ as given by (27); from $\tilde{R} = \tilde{R}_a$ to $\tilde{R} = \tilde{R}_o$, the integration by Simpson's rule continues, using the expression (24) for $\tilde{T} = \tilde{T}^{(1)}$.

5. EXAMPLE: NEO-HOOKEAN MATERIAL

Let it be assumed that the original material of the sphere is a neo-Hookean elastic solid and that the material of each subsequently formed network also exhibits neo-Hookean response. The strain energy density functions $W^{(1)}$ and $W^{(2)}$ for the original and newly formed network materials, respectively, are taken as

$$W^{(1)}(I_1, I_2) = c^{(1)}(I_1 - 3); \quad W^{(2)}(\hat{I}_1, \hat{I}_2) = c^{(2)}(\hat{I}_1 - 3), \tag{48}$$

where $c^{(1)}$ and $c^{(2)}$ are constants interpreted as material moduli. Comparison with (25) and (28) shows that

$$c^{(1)} = E^{(1)} = W_1^{(1)}; \quad c^{(2)} = E^{(2)} = W_1^{(2)}. \tag{49}$$

In the present solution, stress quantities are normalized by the modulus $E^{(1)}$. It is emphasized that the restriction to neo-Hookean network response is not necessary. Both original and subsequently formed materials are taken as neo-Hookean to demonstrate as clearly as possible the effects of the conversion phenomenon itself on overall mechanical response. The possibility is allowed that the original and newly formed materials have different moduli, that is, $E^{(1)}$ and $E^{(2)}$ may not be equal. Let $\tilde{E} = E^{(2)}/E^{(1)}$.

Consider first a monotonic process of increasing λ_i. Figure 2 shows the radial normal stress $\tilde{T}_{rr}$ versus $\tilde{R}$ for various amounts of microstructural conversion C when the deformation control parameter is $\lambda_i = 6.0$. Because $\lambda_a = 1.5$, the dimensionless activation radius is found from (47) to be $\tilde{R} \approx 4.49$. The ratio of moduli of newly

formed networks and original material is $\tilde{E} = 1.0$. For comparison, the results for a neo-Hookean material undergoing no transformation ($C = 0.0$) are plotted by the solid line. The radial stress is seen in all cases to increase monotonically from the value imposed by the inner boundary condition $\tilde{T}_{rr}(1) = 0$. The figure shows that $\tilde{T}_{rr}$ is lower at all $\tilde{R}$ for each value of $C > 0.0$ than is the case when $C = 0.0$. Furthermore, it can be seen that a larger value of C causes the radial stress to be lower for all $\tilde{R}$.

Figure 3 shows plots of the circumferential normal stress $\tilde{T}_{\theta\theta} = \tilde{T}_{\phi\phi}$ versus $\tilde{R}$ for different values of C, with $\tilde{E} = 1.0$. Values were calculated using (26) and (37). The stretch ratio at $\tilde{R} = 1$ in this deformation-control simulation is again taken as $\lambda_i = 6.0$. As has been shown for $\tilde{T}_{rr}$ in Figure 2, Figure 3 shows that $\tilde{T}_{\theta\theta}$ is lower for all $\tilde{R}$ when C is greater. This phenomenon is associated with the conversion-softening of mechanical response implied by the constitutive equation. Figure 3, however, demonstrates more than a simple reduction of $\tilde{T}_{\theta\theta}$ at high values of C: a fundamental change in the stress distribution occurs when greater amounts of conversion are assumed. In the neo-Hookean case with no network scission, $\tilde{T}_{\theta\theta}$ is greatest at the inner surface of the sphere, $\tilde{R} = 1$, and decreases monotonically as $\tilde{R}$ increases to $\tilde{R} = \tilde{R}_o$. When $C = 1.0$, $\tilde{T}_{\theta\theta}(1)$ has been reduced to approximately 10% of the value it holds for $C = 0.0$. $\tilde{T}_{\theta\theta}$ then increases with $\tilde{R}$, reaching a local maximum before decreasing as $\tilde{R}$ goes to $\tilde{R} = \tilde{R}_o$. These results show that the constitutive equation for materials undergoing microstructural change implies stress relief nearest the inner surface of the sphere: deformation there is greatest; microstructural transformation is greatest at large deformation; the reduction of stress compared to the elastic response is greatest when the most transformation has occurred.

Figure 4 shows $\tilde{T}_{\theta\theta}$ versus $\tilde{R}$ for three values of the deformation control parameter λ_i, with $C = 1.0$ and $\tilde{E} = 1.0$. Note that the vertical scale differs from that of Figure 3. The stress is significantly lower near $\tilde{R} = 1$ when $\lambda_i = 6.0$ than when $\lambda_i = 4.0$. Thus a process of increasing deformation results in decreasing circumferential stress nearest the inner surface of the sphere when a large amount of conversion is assumed.

Figure 5 shows the external traction $\tilde{T}_o$ versus λ_i for three values of the ratio of moduli $\tilde{E}$. The conversion fraction is taken as $C = 1.0$. For comparison, the neo-Hookean case with $C = 0.0$ is represented by the solid curve. It can be seen from the figure that the external traction associated with a given value of the deformation control parameter λ_i is smaller when conversion is assumed than in the purely elastic case. It may be said in general that conversion leads to a softening of the response of the sphere for $\lambda_i \geq \lambda_a$. Figure 5 indicates that variations of the modulus ratio over the range $\tilde{E} \in [0.5, 2.0]$ used in this work have little noticeable influence on the $\tilde{T}_o$-λ_i relation. For this reason, no further comparisons of response for different values of $\tilde{E}$ are presented in this article. The value $\tilde{E} = 1.0$ is used henceforth.

Figure 6 shows the $\tilde{T}_o$-λ_i relation for different values of C. The softening effect is evident for $\lambda_i > \lambda_a = 1.5$ for each value of $C > 0.0$ shown and is more pronounced when C is larger. It may be noted that the values of $\tilde{T}_o$ for $\lambda_i = 6.0$ correspond to the values of $\tilde{T}_{rr}$ given in Figure 2 for $\tilde{R} = \tilde{R}_o = 10$.

All of the curves plotted in Figure 6 demonstrate nonmonotonic $\tilde{T}_o$-λ_i relations. Indeed, Carroll [12] has shown that, for a sphere of a neo-Hookean material and any

(text continues on page 288)

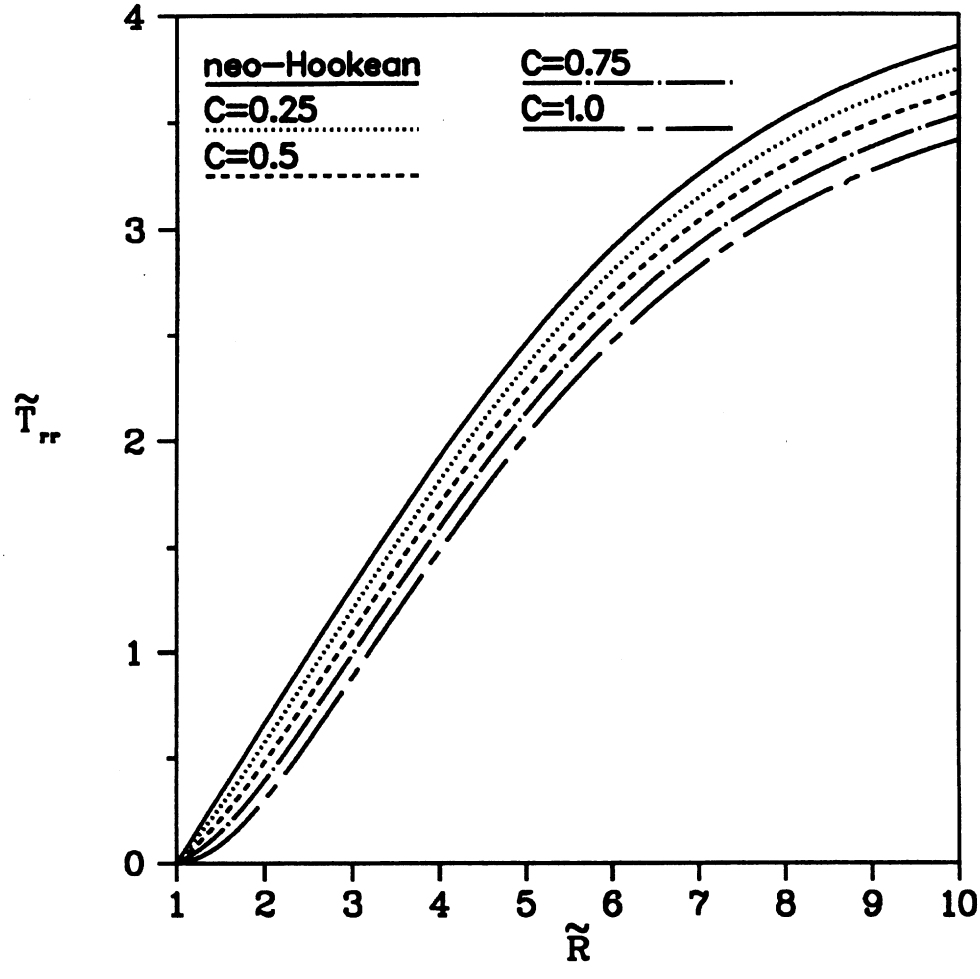

Fig. 2. Radial stress versus radius for various conversion fractions (λ_i increasing), with $\tilde{R}_o = 10$, $\lambda_i = 6.0$, $\tilde{E} = 1.0$, $\lambda_a = 1.5$, and $\lambda_c = 6.1$.

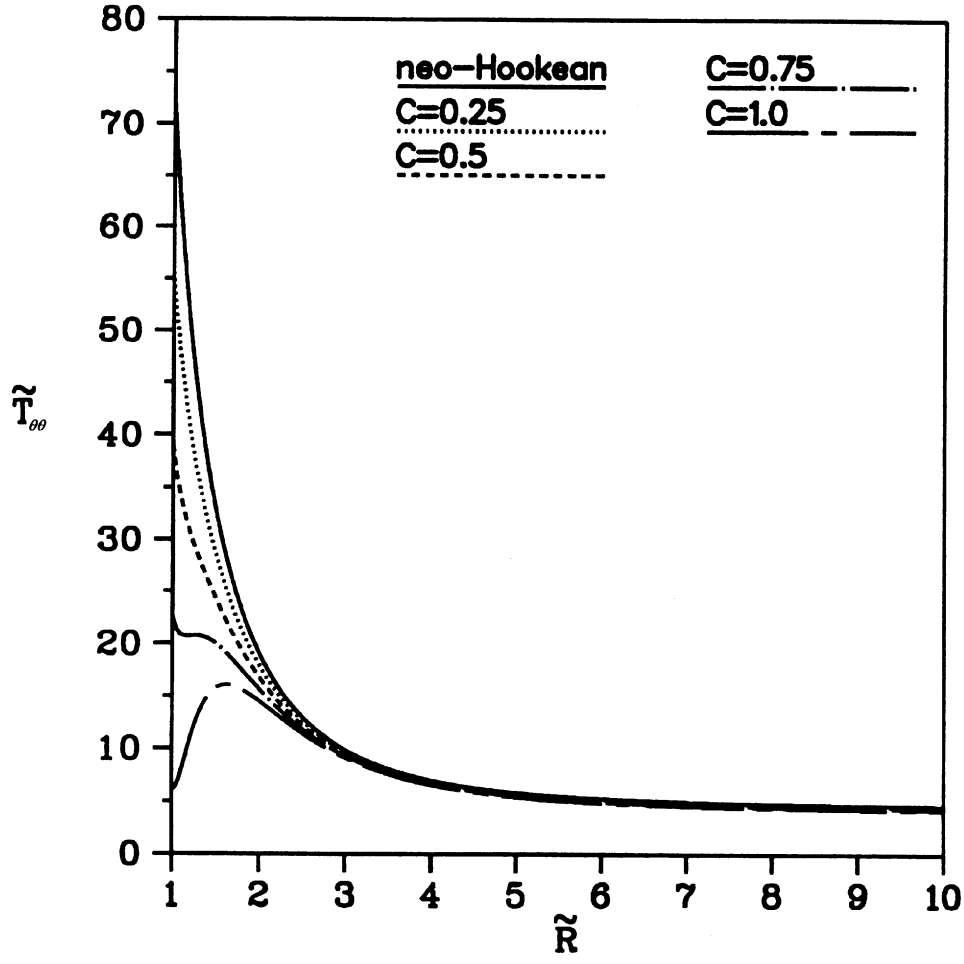

Fig. 3. Circumferential stress versus radius for various conversion fractions (λ_i increasing), with $\tilde{R}_o = 10$, $\lambda_i = 6.0$, $\tilde{E} = 1.0$, $\lambda_a = 1.5$, and $\lambda_c = 6.1$.

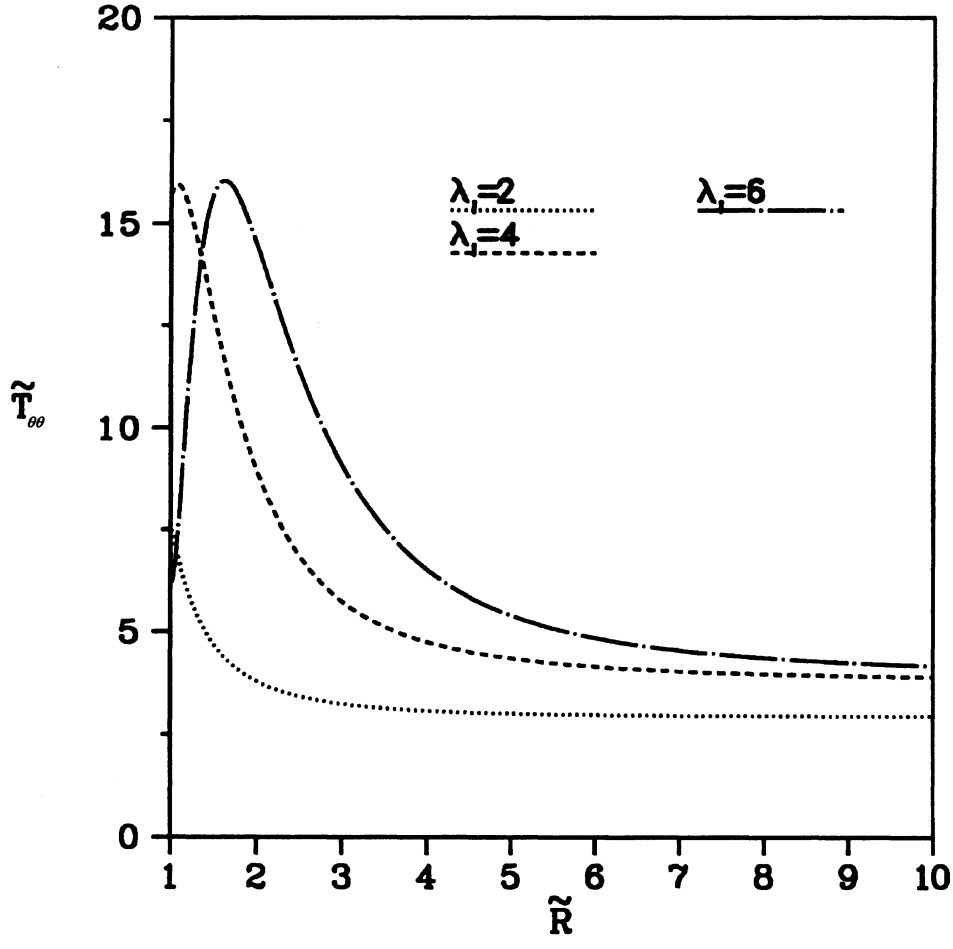

Fig. 4. Circumferential stress versus radius for various inner surface stretch ratios (λ_i increasing), with $\tilde{R}_o = 10$, $C = 1.0$, $\tilde{E} = 1.0$, $\lambda_a = 1.5$, and $\lambda_c = 6.1$.

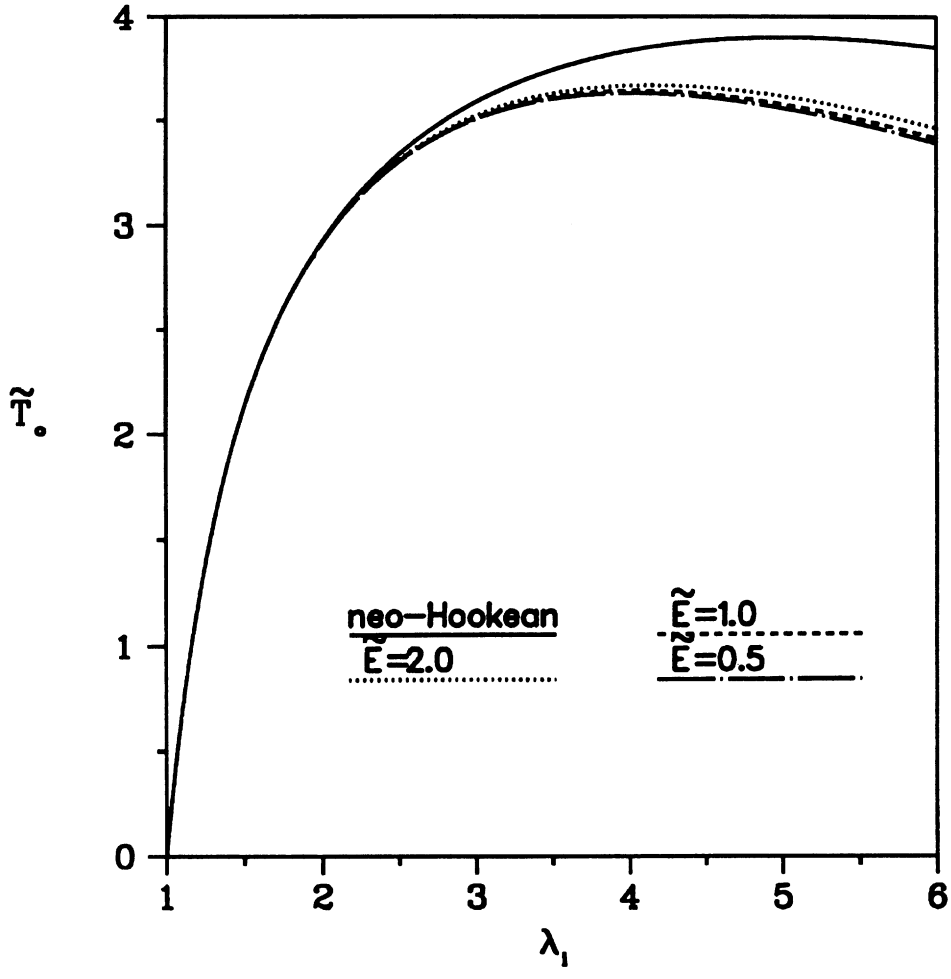

Fig. 5. External radial tensile traction versus inner surface stretch ratio for various extension modulus ratios (λ_i increasing), with $\tilde{R}_o = 10$, $C = 1.0$, $\lambda_a = 1.5$, and $\lambda_c = 6.1$.

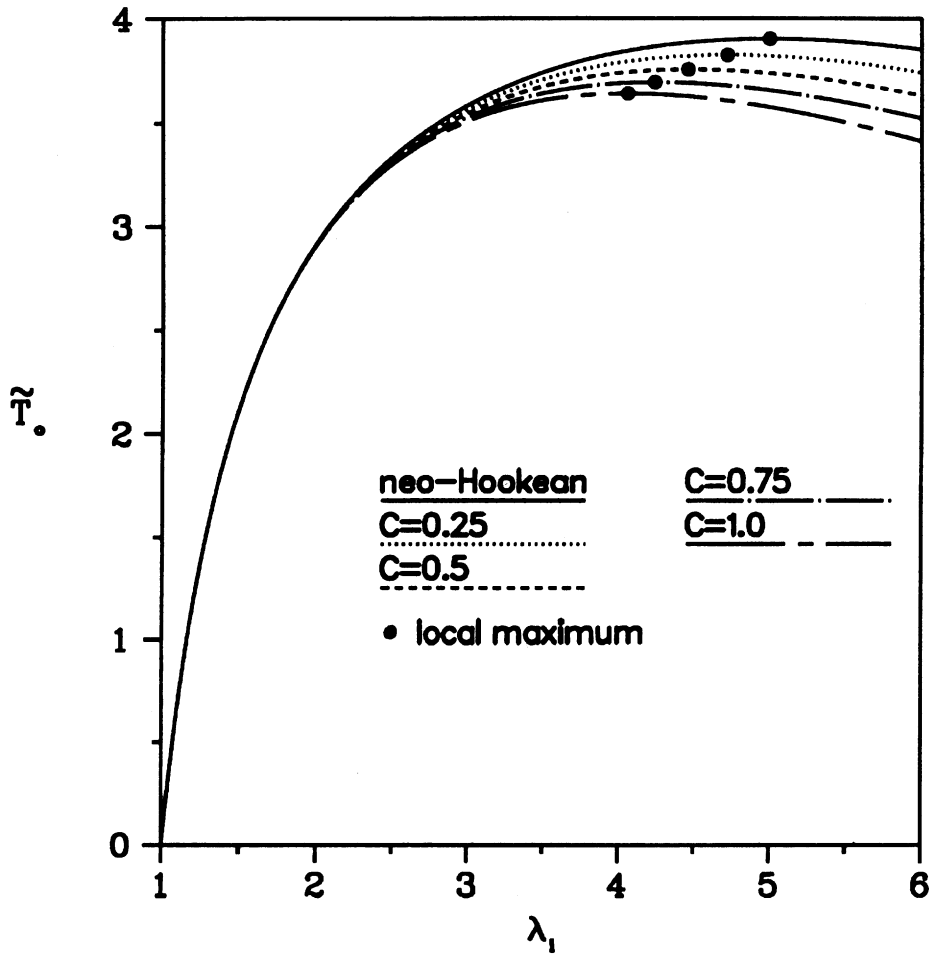

Fig. 6. External radial tensile traction versus inner surface stretch ratio for various conversion fractions (λ_i increasing), with $\tilde{R}_o = 10$, $\tilde{E} = 1.0$, $\lambda_a = 1.5$, and $\lambda_c = 6.1$.

normalized thickness $\tilde{R}_o$, a loss of monotonicity will occur at some λ_i. It has been seen from Figures 2 and 3 that all of the values of C selected for plotting have implied cases of conversion-softening. The effect is evident in Figure 6. The local maximum of $\tilde{T}_o$, indicated on each curve by a heavy dot, can be seen to occur at smaller λ_i when C is greater. The critical value of λ_i decreases from $\lambda_i^{cr} \approx 5.00$ for the neo-Hookean material to $\lambda_i^{cr} \approx 4.06$ when $C = 1.0$. The external traction associated with λ_i^{cr} decreases from $\tilde{T}_o^{cr} \approx 3.90$ to $\tilde{T}_o^{cr} \approx 3.64$. A thorough discussion of the influence of the constitutive model on the $\tilde{T}_o$-λ_i relation has been provided by [6].

Assume now that the sphere has undergone a process of increasing λ_i such that the maximum value of the deformation control parameter reached is $\lambda_i^* \geq \lambda_a$. The maximum value of the activation radius $\tilde{R}_a$ reached during this process is found from

(47) to be

$$\tilde{R}_a^* = \left(\frac{\lambda_i^{*3} - 1}{\lambda_a^3 - 1} \right)^{\frac{1}{3}}. \tag{50}$$

Let $\lambda^*(\tilde{R})$ denote the stretch ratio distribution when $\lambda_i = \lambda_i^*$. It is formed from (46) as

$$\lambda^*(\tilde{R}) = \left(1 + \frac{\lambda_i^{*3} - 1}{\tilde{R}^3} \right)^{\frac{1}{3}}. \tag{51}$$

Assume that λ_i is subsequently reduced from λ_i^*. Figure 7 reproduces from Figure 6 the $\tilde{T}_o$-λ_i curves for various values of the conversion fraction C during a process of increasing deformation. Superposed are the corresponding $\tilde{T}_o$-λ_i curves for a reduction of deformation from $\lambda_i^* = 5.0$ to $\lambda_i = \lambda_i^{res}$, the value of the control parameter defined by $\tilde{T}_o(\lambda_i^{res}) = 0$. It is seen that the value of the external traction associated with any value of λ_i given by $\lambda_i' \in [\lambda_i^{res}, \lambda_i^*]$ during the reduction of deformation is less than $\tilde{T}_o(\lambda_i')$ during the process of increasing deformation. As deformation is reduced, the slope of the T_o-λ_i curve near $\lambda_i = \lambda_a = 5.0$ indicates that large amounts of deformation recovery occur early in the process and correspond to relatively small changes in the external traction. Figure 7 shows that, for the present choice of geometric and conversion parameters, the $\tilde{T}_o$-λ_i curve remains monotonic for all values of C as deformation is decreased.

From Figure 7, a residual deformation λ_i^{res} can be seen at $\tilde{T}_o = 0$ after deformation has been reduced from $\lambda_i^* = 5.0$. Figure 8 shows plots of λ_i^{res} versus λ_i^* for different values of C. When $\lambda_i^* < \lambda_a = 1.5$, there is no residual deformation. The residual stretch ratio λ_i^{res} increases with λ_i^* for $\lambda_i^* > 1.5$. The residual stretch λ_i^{res} can also be seen to be greater for all $\lambda_i^* > 1.5$ when the maximum possible conversion fraction C is larger. Greater amounts of network scission and reconstruction lead to greater permanent set of the sphere.

Figure 9 shows the residual radial stress distribution $\tilde{T}_{rr}^{res}(\tilde{R})$ when deformation is decreased from various values of λ_i^*. The conversion fraction is taken as $C = 1.0$. In all cases, the residual stress $\tilde{T}_{rr}^{res}$ is everywhere compressive. The compressive residual radial stress near $\tilde{R} = 1.0$ increases as λ_i^* increases. Figure 10 shows plots of $\tilde{T}_{rr}^{res}$ versus $\tilde{R}$ for several values of C when deformation is reduced from $\lambda_i^* = 5.0$. For any amount of network conversion, the residual radial stress is again compressive for all $\tilde{R}$. As the parameter C is increased, the magnitude of this compressive stress increases for all $\tilde{R}$. In both Figure 9 and 10, an internal region of high radial compressive stress can be seen near $\tilde{R} = 2$.

Figure 11 shows the residual circumferential stress distribution $\tilde{T}_{\theta\theta}^{res}(\tilde{R})$ for different values of λ_i^* when $C = 1.0$. Comparison of Figure 11 and Figure 9 reveals that the magnitude of $\tilde{T}_{\theta\theta}^{res}$ is in general greater than that of $\tilde{T}_{rr}^{res}$. The striking feature of Figure 11 is a relatively thin region of material near $\tilde{R} = 1$ where $\tilde{T}_{\theta\theta}^{res} < 0$. When the deformation of the sphere is reduced from a greater value of λ_i^*, the boundary of this compressive layer moves outward; the magnitude of the compressive stress also increases everywhere within the layer. Figure 12 shows $\tilde{T}_{\theta\theta}^{res}$ versus $\tilde{R}$ for various C, with

(text continues on page 293)

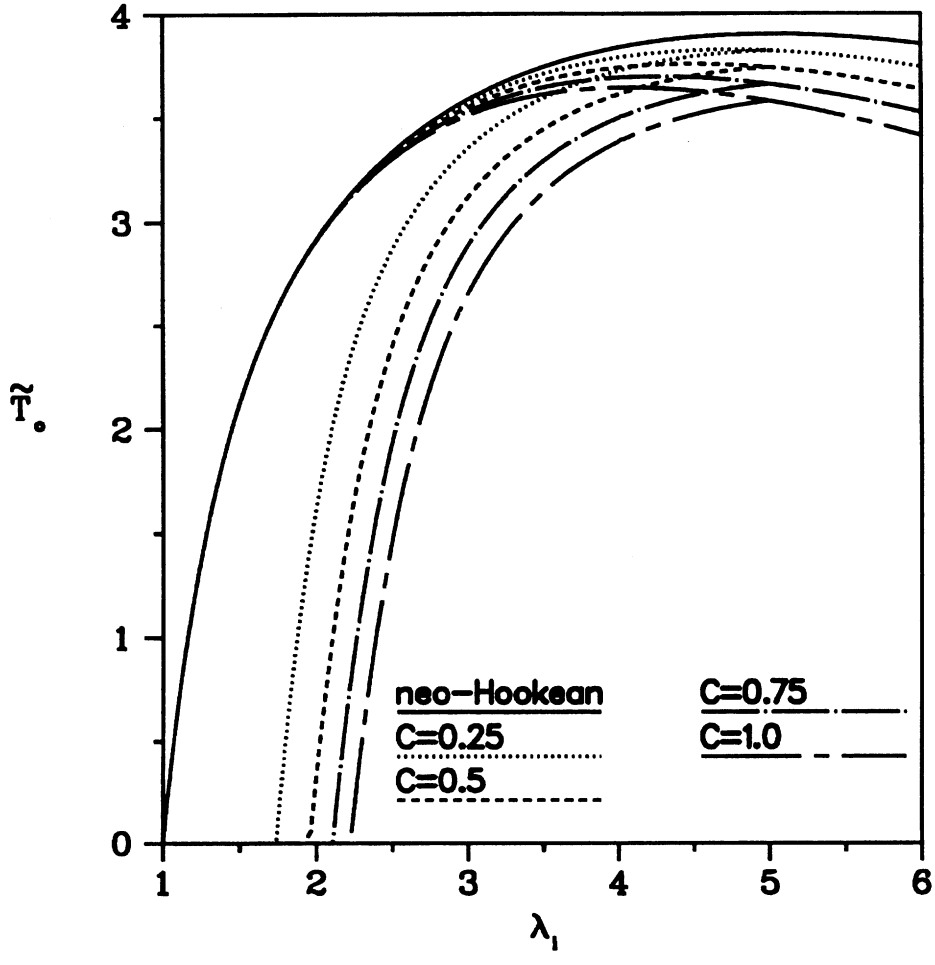

Fig. 7. External radial tensile traction versus inner surface stretch ratio for various conversion fractions (λ_i increasing, then decreasing), with $\tilde{R}_o = 10$, $\tilde{E} = 1.0$, $\lambda_a = 1.5$, and $\lambda_c = 6.1$.

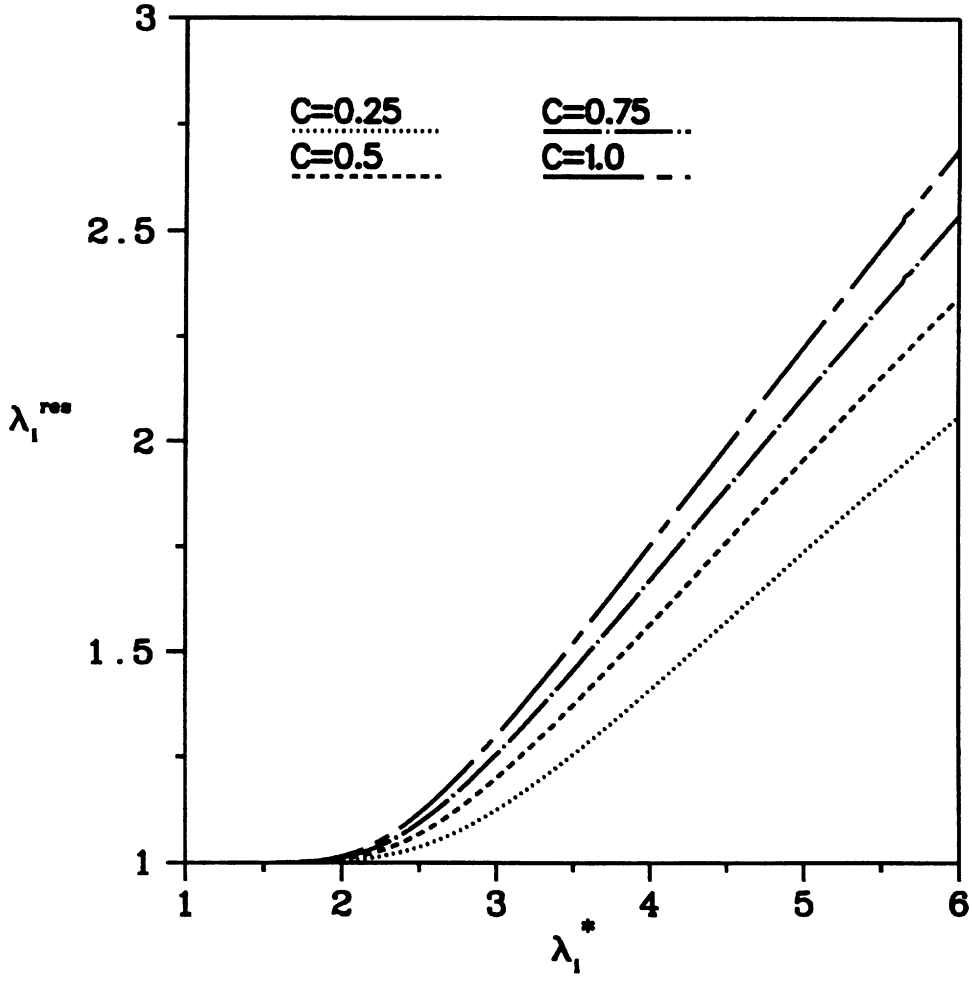

Fig. 8. Residual inner surface stretch ratio versus maximum stretch ratio for various conversion fractions, with $\tilde{R}_o = 10$, $\tilde{E} = 1.0$, $\lambda_a = 1.5$, and $\lambda_c = 6.1$.

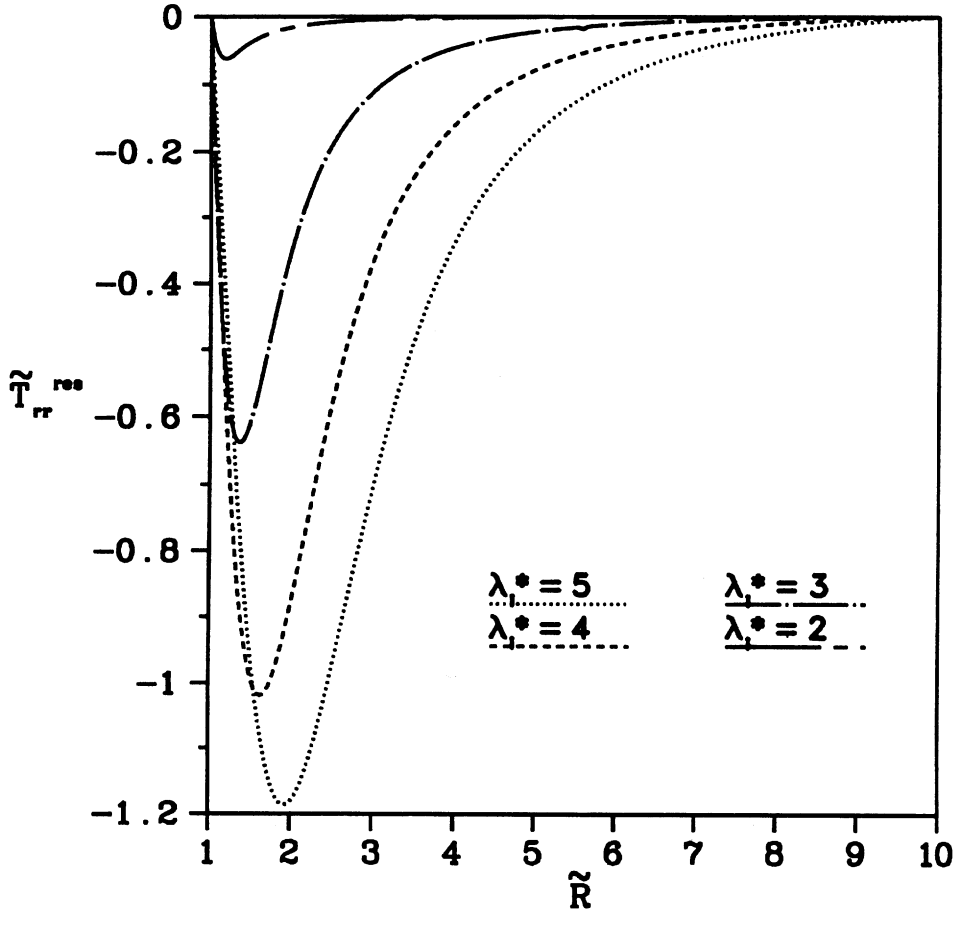

Fig. 9. Residual radial stress versus radius for various maximum inner surface stretch ratios, with $\tilde{R}_o = 10$, $C = 1.0$, $\tilde{E} = 1.0$, $\lambda_a = 1.5$, and $\lambda_c = 6.1$.

$\lambda_i^* = 5.0$. It can be seen that the outer boundary of the residual compressive layer varies only slightly as different amounts of conversion C are assumed. Yet the magnitude of the stress increases for all R within the compressive region as C is increased. Thus any amount of conversion assumed leads to the formation of a residual compressive layer of nearly constant thickness; the assumption of a greater amount of conversion intensifies the stress within this layer.

6. REMARKS ON SPECIAL CASES

6.1. Membrane

There exist experimentally convenient configurations for the measurement of the present spherical deformation. One such configuration is the inflation of a spherical balloon by a uniform internal pressure p_i. It is easily shown that the T_o-λ_i relation is equivalent to the p_i-λ_i relation for incompressible materials. Thus the internal pressurization of a hollow sphere may be considered within the framework already established for the study of the deformation of a hollow sphere by a uniform radial tensile traction.

The present work has considered only the exact formulation of the boundary-value problem, with emphasis on the variation of stresses and of microstructural conversion through the thickness of the sphere. The inflation of a spherical balloon, however, would be analyzed most naturally using the approximations of membrane theory, whereby all stresses, material properties and conversion behavior would be regarded as constant throughout the thickness of the membrane. With $R_o/R_i \approx 1$, it can be seen from (16) that the initial radial position of all material particles can be approximated by a coordinate $\bar{R}$ and the current radial position by a coordinate $\bar{r}$. A single stretch ratio $\bar{\lambda} = \bar{r}/\bar{R}$ would approximate the deformation of all material.

It is not the aim of this work to formulate an approximate theory for use in the balloon inflation problem. Nonetheless, the nature of the results that would be obtained can be appreciated within the context of the present formulation by numerical simulation with $\tilde{R}_o \approx 1$. Figure 13 shows T_o versus λ_i for neo-Hookean network materials when $\tilde{R}_o = 1.05$. Shown are curves for increasing deformation and for deformation decreasing from $\lambda_i^* = 5.0$. The parameters $C = 1.0$, $\tilde{E} = 1.0$, $\lambda_a = 1.5$ and $\lambda_c = 6.1$ are used.

Hart-Smith [13] and Beatty [14] have published results of experimental measurement of inflating pressure versus stretch for balloons. It is encouraging that their plots display some of the general features evident in Figure 13: (a) deformation decreases along a different path from that of increasing deformation; (b) residual deformation or permanent set is seen when the inflating pressure has been returned to zero. Comparison of Hart-Smith's and Beatty's measurements with the results of numerical simulations such as those shown in Figure 13 could provide a starting point for the verification or correction of the constitutive equation for materials undergoing microstructural transformation in equal biaxial extension. Experimental programs providing further data for other materials would support this effort.

(text continues on page 298)

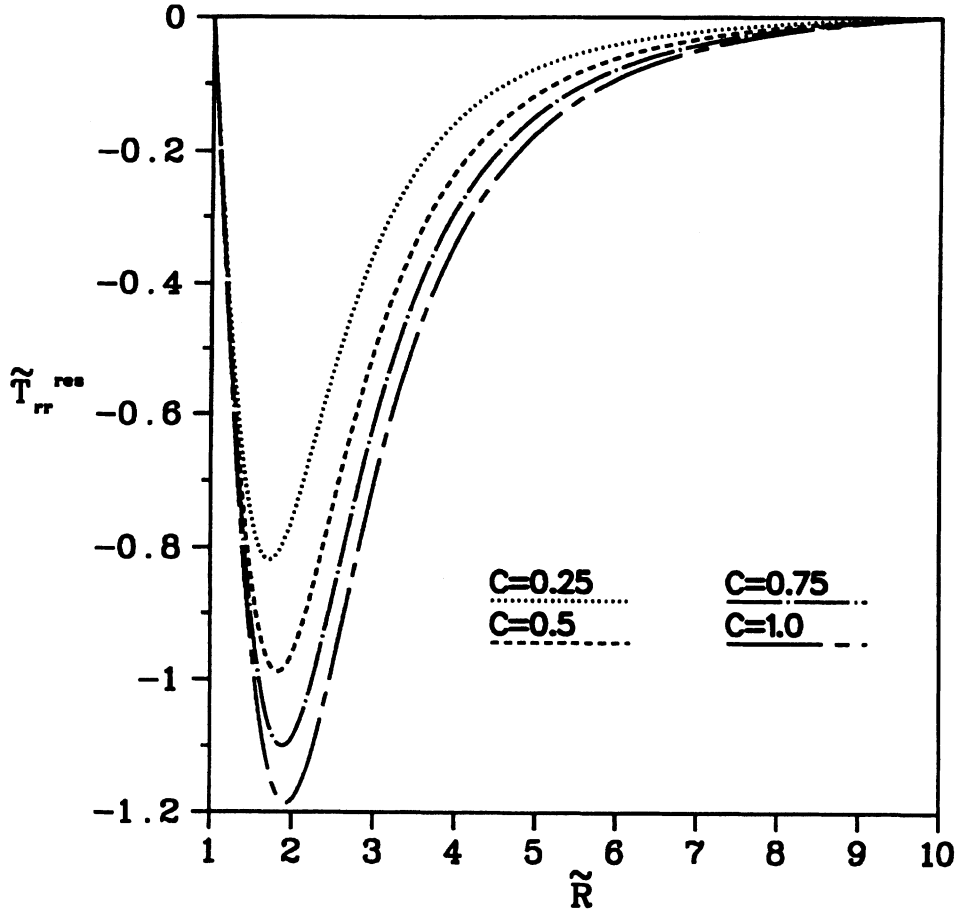

Fig. 10. Residual radial stress versus radius for various conversion fractions, with $\tilde{R}_o = 10$, $\lambda_i^* = 5.0$, $\tilde{E} = 1.0$, $\lambda_a = 1.5$, and $\lambda_c = 6.1$.

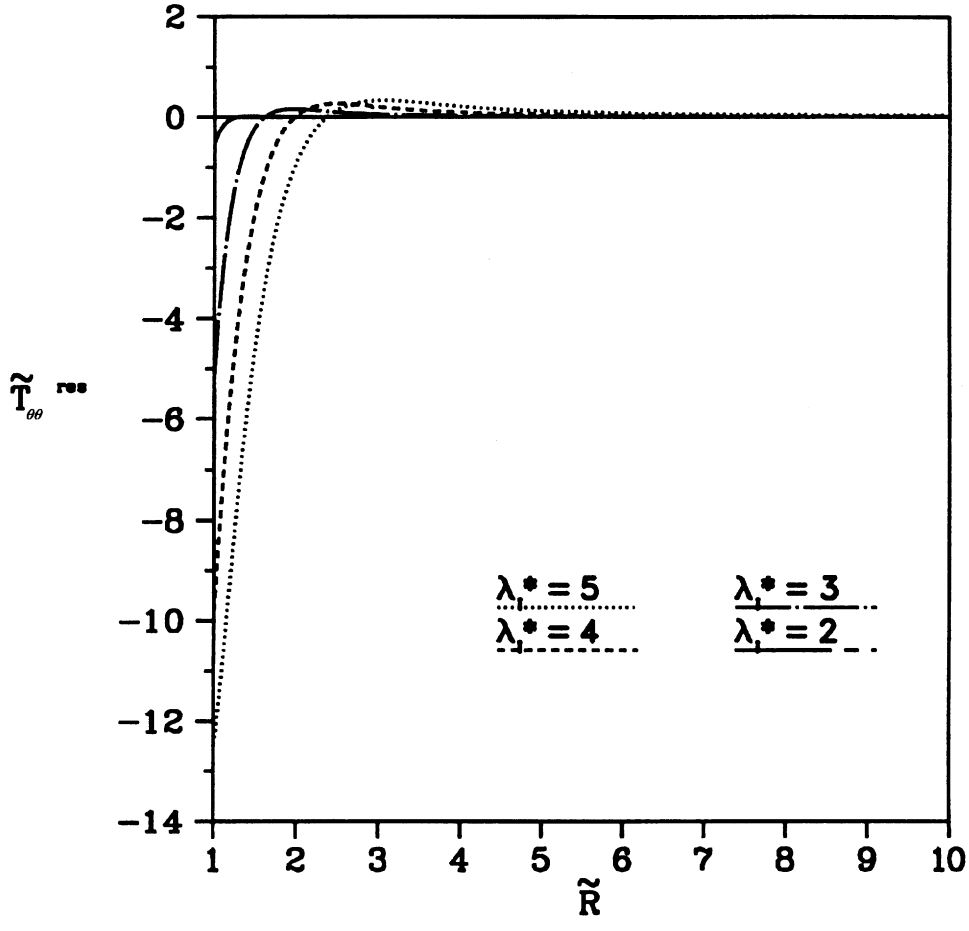

Fig. 11. Residual circumferential stress versus radius for various maximum inner surface stretch ratios, with $\tilde{R}_o = 10$, $C = 1.0$, $\tilde{E} = 1.0$, $\lambda_a = 1.5$, and $\lambda_c = 6.1$.

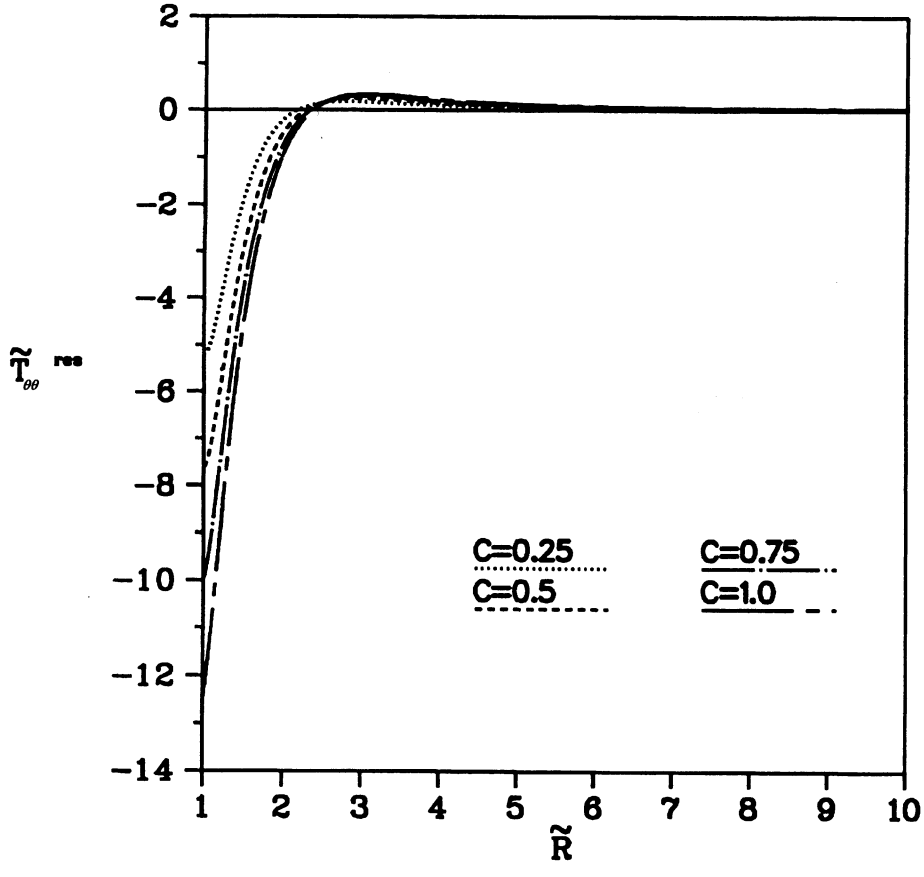

Fig. 12. Residual circumferential stress versus radius for various conversion fractions, with $\tilde{R}_o = 10$, $\lambda_i^* = 5.0$, $\tilde{E} = 1.0$, $\lambda_a = 1.5$, and $\lambda_c = 6.1$.

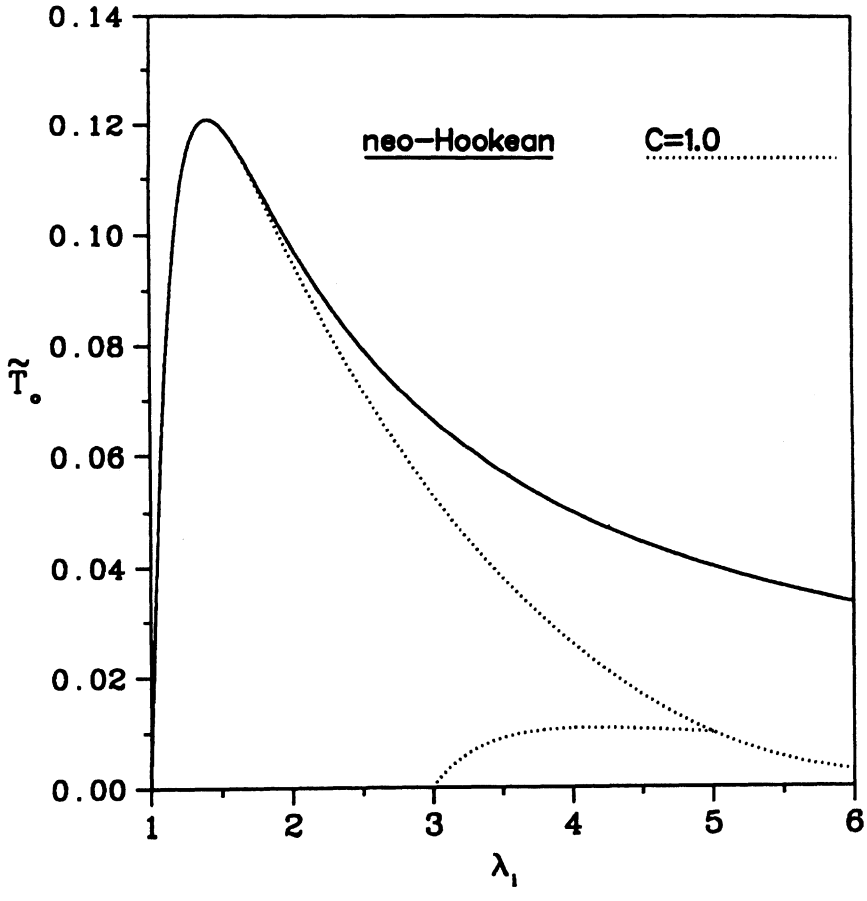

Fig. 13. External radial tensile traction versus inner surface stretch ratio (λ_i increasing, then decreasing), with $\tilde{R}_o = 1.05$ (membrane), $C = 1.0$, $\tilde{E} = 1.0$, $\lambda_a = 1.5$, and $\lambda_c = 6.1$.

6.2. Microvoid

With the assumption $\tilde{R}_o \gg 1$, the geometry and loading considered in this paper can be applied to simulate a microvoid at the center of a large spherical specimen under uniform radial tensile loading. Studying this case in the context of finite deformation is imperative, as the equal biaxial stretch ratio at the boundary of the microvoid can become extremely large even when the deformation of the outer surface of the specimen is small. For example, with $\tilde{R}_o = 100$, it can be seen from (46) that a stretch ratio $\lambda_i = 10.0$ at the boundary of the micro-void is associated with a stretch ratio of only $\lambda_o \approx 1.00033$ at the outer surface of the specimen. (A similar phenomenon has been noted experimentally by Sue and Yee [15], who observed very large strains in the neighborhood of rigid inclusions in nylon specimens subjected to moderate deformation.) Deformation near a microvoid can become so large that the applicability of many purely elastic theories must be called into question (Alexander [16]; Treloar [17]). It seems reasonable to apply to this geometry a constitutive equation that allows for microstructural change at large deformation.

The general features of the results presented in Section 5 for the neo-Hookean material with $\tilde{R}_o = 10$ also apply when $\tilde{R}_o = 100$. However, one important difference should be noted. The activation value $\lambda_a = 1.5$ is used to obtain the results presented in Section 5; $\lambda_i = 6.0$ is the largest inner stretch ratio considered in that section. With these values, the activation radius can be found from (47) to be $\tilde{R}_a \approx 4.49$. This value is independent of $\tilde{R}_o$. Recall that the activation radius represents the outermost spread of microstructural transformation through the sphere; thus the effects of the conversion process are localized in a very thin layer of material nearest the microvoid. To see some of these effects, refer to the distributions of the circumferential stress $\tilde{T}_{\theta\theta}(\tilde{R})$, shown in Figures 3 and 4, and of the residual radial and circumferential stresses $\tilde{T}^{res}_{rr}(\tilde{R})$ and $\tilde{T}^{res}_{\theta\theta}(\tilde{R})$ in Figure 9 through Figure 12. In a sphere-microvoid system with $\tilde{R}_o = 100$, the distributions are very similar to those mentioned above for $\tilde{R}_o = 10$. They indicate extremely localized concentrations of large stresses in the material immediately surrounding the microvoid.

The T_o-λ_i relation describes the size of the microvoid associated with an applied external traction. Non-monotonicity of this relation can indicate unstable growth of the microvoid as the external traction increases. When the sphere is assumed to be composed of a neo-Hookean material undergoing no transformation and $\tilde{R}_o = 100$ is prescribed, a local maximum of T_o in λ_i arises at $\lambda_i \approx 22.77$. If it is possible that the material deforms to such a stretch ratio in equal biaxial extension, it may not remain perfectly elastic. The constitutive equation for microstructural change may better represent physical events leading to unstable void growth. Indeed, it has been seen in Figure 6 that softening of response due to network conversion can in general bring about a local maximum in T_o at a lower value of λ_i than is the case when no conversion occurs. A constitutive equation, which predicts a loss of monotonicity at stretch ratios that are more likely to be realized, may aid in the study of the growth of microvoids.

Considerable attention has been devoted recently to the growth of microvoids in elastic materials (Horgan and Pence [18,19]; Chou-Wang and Horgan [20]). Of particu-

lar interest is work by [18] on composite spheres. The spheres consist of distinct inner and outer regions: Both regions are assumed to be neo-Hookean, but their moduli differ. Horgan and Pence showed that variations in the relative moduli of the inner and outer regions can influence the growth of a microvoid. In particular, the level of deformation and the associated external traction at which unstable growth is initiated are affected. This application of the constitutive equation for materials undergoing microstructural transformation to the sphere problem represents a natural extension of that work.

REFERENCES

[1] Rajagopal, K. R. and Wineman, A. S.: A constitutive equation for nonlinear solids which undergo deformation induced microstructural changes. *Int. J. Plast.*, 8, 385-395 (1992).

[2] Tobolsky, A. V.: *Properties and Structure of Polymers*, John Wiley, New York, 1960.

[3] Wineman, A. S. and Rajagopal, K. R.: On a constitutive theory for materials undergoing microstructural changes. *Arch. Mech.*, 42, 1, 53-75 (1990).

[4] Huntley, H. E.: Applications of a constitutive equation for microstructural change in polymers, Ph.D. dissertation, The University of Michigan, 1992.

[5] Wineman, A. S. and Huntley, H. E.: Numerical simulation of the effect of damage induced softening on the inflation of a circular rubber membrane. *Int. J. Solids Structures*, 31, 23, 3295-3313 (1994).

[6] Huntley, H. E., Wineman, A. S., and Rajagopal, K. R.: Load maximum behavior in the inflation of hollow spheres of incompressible material with strain-dependent damage, unpublished manuscript, 1995.

[7] Rajagopal, K. R. and Srinivasa, A. R.: On the inelastic behavior of solids, part I: Twinning. *Int. J. Plast.*, 11, 653-678 (1995a).

[8] Rajagopal, K. R. and Srinivasa, A. R.: Inelastic behavior of materials, part II: Energetics associated with discontinuous twinning, unpublished manuscript, 1995b.

[9] Spencer, A.J.M.: *Continuum Mechanics*, Longman Mathematical Texts, New York, 1980.

[10] Rajagopal, K. R.: On constitutive relations and material modelling in continuum mechanics, Report #6, Institute for Applied and Computational Mechanics, The University of Pittsburgh, 1995.

[11] Carroll, M. M.: Controllable deformations of incompressible simple materials. *Int. J. Eng. Sci.*, 5, 515-525 (1967).

[12] Carroll, M. M.: Pressure maximum behavior in inflation of incompressible elastic hollow spheres and cylinders. *Quarterly of Applied Mathematics*, 45, 1, 141-154 (1987).

[13] Hart-Smith, L. J.: Elasticity parameters for finite deformations of rubber-like materials. *Zeitschrift für Angewandte Mathematik und Physik*, 17, 608-625 (1966).

[14] Beatty, M. F.: Topics in finite elasticity: Hyperelasticity of rubber, elastomers, and biological tissues–With Examples. *Appl. Mech. Rev.*, 40, 12, 1699-1734 (1987).

[15] Sue, H.-J. and Yee, A. F.: Toughening mechanisms in a multi-phase alloy of nylon 6,6/polyphenylene oxide. *J. Mat. Sci.*, 24, 1447-1457 (1989).

[16] Alexander, H.: A constitutive relation for rubber-like materials. *Int. J. Eng. Sci.*, 6, 549-563 (1968).

[17] Treloar, L.R.G.: *The Physics of Rubber Elasticity*, 3rd ed., Oxford University Press, Oxford, UK, 1975.

[18] Horgan, C. O. and Pence, T. J.: Void nucleation in tensile dead-loading of a composite incompressible nonlinearly elastic sphere. *J. Elast.*, 21, 61-82 (1989a).

[19] Horgan, C. O. and Pence, T. J.: Cavity formation at the center of a composite incompressible nonlinearly elastic sphere. *Trans. ASME*, 56, 302-308 (1989b).

[20] Chou-Wang, M.-S. and Horgan, C. O.: Void nucleation and growth for a class of incompressible nonlinearly elastic materials. *Int. J. Solids Structures*, 25, 11, 1239-1254 (1989).